CHAPTER III

RESULTS

3.1 Clinical features

Forty-five cases of PBL were included in the study. The group consisted of 31 males, 12 females and 2 of unknown gender. Two patients were white males, 1 was of unknown race and the rest were black patients. The male to female ratio was 2.6:1. The mean age of the patients was 41 years (29-58 years). The gingiva as well as the buccal vestibule and palate were the most commonly affected intra-oral areas. The HIV-status of 13 patients was unknown, 31 were HIV positive and 1 was HIV negative (Table 2).

Table 2: *The table represents a summary of the clinical features of all PBL cases included in the study*

Case	Age	Race	Sex	HIV status	Anatomical Location
1	47	B	M	+	Gingiva posterior maxilla
2	48	B	M	+	Gingiva posterior mandible & sulcus
3	34	B	F	+	Gingiva posterior mandible
4	52	B	F	+	Buccal sulcus
5	U	B	M	+	Gingiva unknown location
6	U	B	U	+	Gingiva maxilla
7	45	B	F	+	Buccal mucosa
8	48	W	M	U	Palate
9	39	B	F	+	Gingiva posterior mandible
10	33	B	F	+	Swelling of face
11	34	B	M	+	Buccal mucosa & soft palate
12	36	B	F	+	Buccal & palate mucosa
13	39	B	M	+	Gingiva unknown location
14	43	B	M	+	Palate, buccal vestibulum
15	28	B	F	+	Gingiva mandible
16	50	B	M	+	Gingiva maxilla
17	36	B	F	-	Gingiva mandible
18	37	B	M	+	Gingiva mandible
19	44	B	M	+	Gingiva mandible
20	45	B	M	U	Gingiva mandible
21	32	B	F	U	Gingiva maxilla & palate
22	45	B	M	U	Palate
23	35	B	M	U	Sockets of teeth 37-38
24	29	B	M	U	Palate
25	44	B	M	U	Gingiva mandible
26	43	B	M	U	Gingiva maxilla
27	45	B	M	U	Gingiva mandible
28	58	B	F	U	Palate
29	43	B	M	+	Gingiva maxilla
30	35	B	M	U	Gingiva anterior mandible
31	39	B	M	+	Gingiva mandibular molar
32	39	B	M	+	Buccal sulcus left
33	50	B	M	+	Maxilla & buccal mucosa
34	U	U	U	+	Gingiva mandible & buccal mucosa
35	U	B	M	+	Gingiva maxilla
36	43	B	M	+	Gingiva left mandible
37	U	B	M	U	Gingiva mandibular retromolar area
38	27	B	M	+	Buccal mucosa
39	36	B	M	+	Gingiva post maxilla & palate
40	40	B	M	U	Gingiva maxilla
41	32	B	M	+	Gingiva unknown location
42	43	W	M	+	Gingiva unknown location
43	45	B	F	+	Gingiva maxilla
44	U	B	F	+	Gingiva mandible
45	44	B	M	+	Gingiva maxilla

B = black; W = white; U = unknown; M = male; F = female

3.2 Microscopic features

Morphologically, all cases showed dense infiltrates of mostly monomorphic, large blastic cells growing in a cohesive, sheet-like pattern (Figs.2 & 3). Some cases showed discohesion between the tumour cells (Fig.4). Tumour cells had either a single prominent nucleolus (Fig.2) (immunoblastic appearance) or several nucleoli (Fig.3) in round to oval eccentrically placed nuclei (plasmablastic appearance). Binucleate and multinucleated tumour cells were sometimes seen focally (Fig.5). In some cases, the tumour cells exhibited prominent pleomorphism with a mixture of blastic cells and cells with large nuclei, either slightly indented or sometimes binucleate (Fig.5). Tumour cells always had abundant cytoplasm with occasional prominent paranuclear hof. Numerous tingible body macrophages imparting a starry sky appearance on microscopic examination were always present (Fig.6). Using the above criteria, 14/45 (31%) of cases were classified as 'PBL with plasmacytic differentiation' based on the presence of more mature plasmacytic cells intermingled with the blasts (Fig.7). Thirty one cases (69%) showed more of the features defining 'PBL of the oral mucosa type' consisting mostly of large blastic cells with much fewer plasmacytic cells (Fig.2). In all cases however, more mature-appearing plasma cells could be identified although the percentage of these cells varied amongst cases examined.

Figure 2: *A case of PBL where almost all of the tumour cells exhibit prominent immunoblastic morphology with a single prominent nucleolus (H&E, 2µm section, original magnification: 400X).*

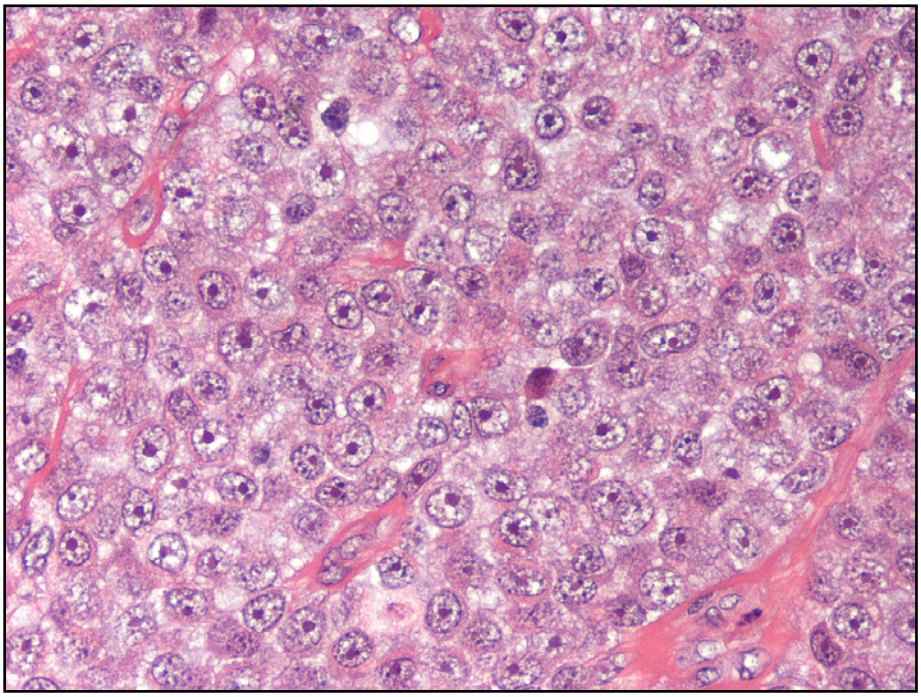

Figure 3: *A case of PBL where all of the tumour cells have a plasmablastic appearance with the tumour cell nuclei exhibiting several nucleoli in large eccentric nuclei (H&E 2µm section, original magnification: 400X).*

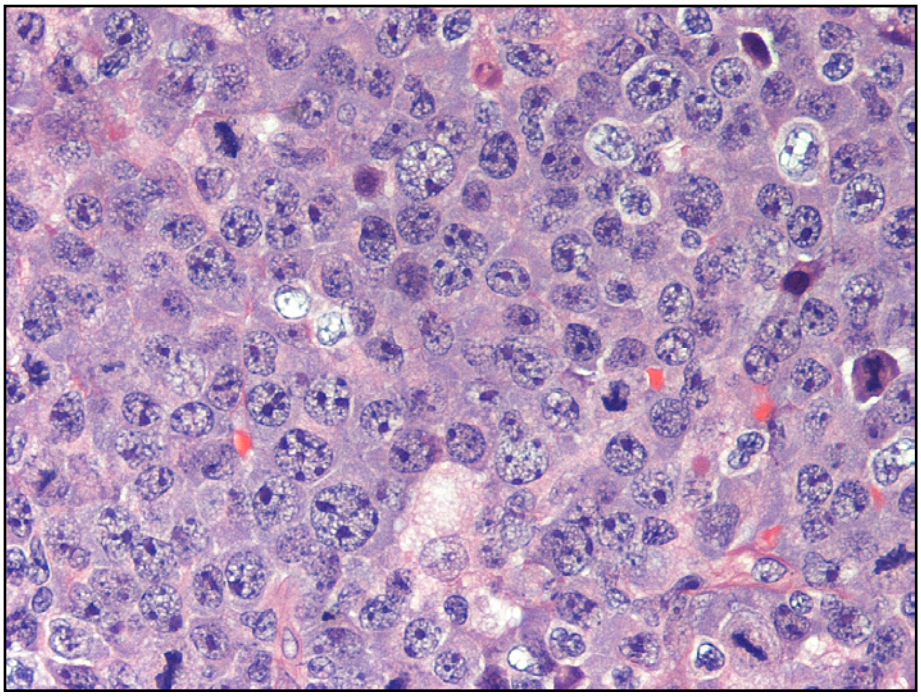

Figure 4: *This photo shows a case of PBL with prominent discohesion (arrows) between the tumour cells. Erythrocytes fill the spaces between the tumour cells (H&E 2µm section; Original magnification: 400X).*

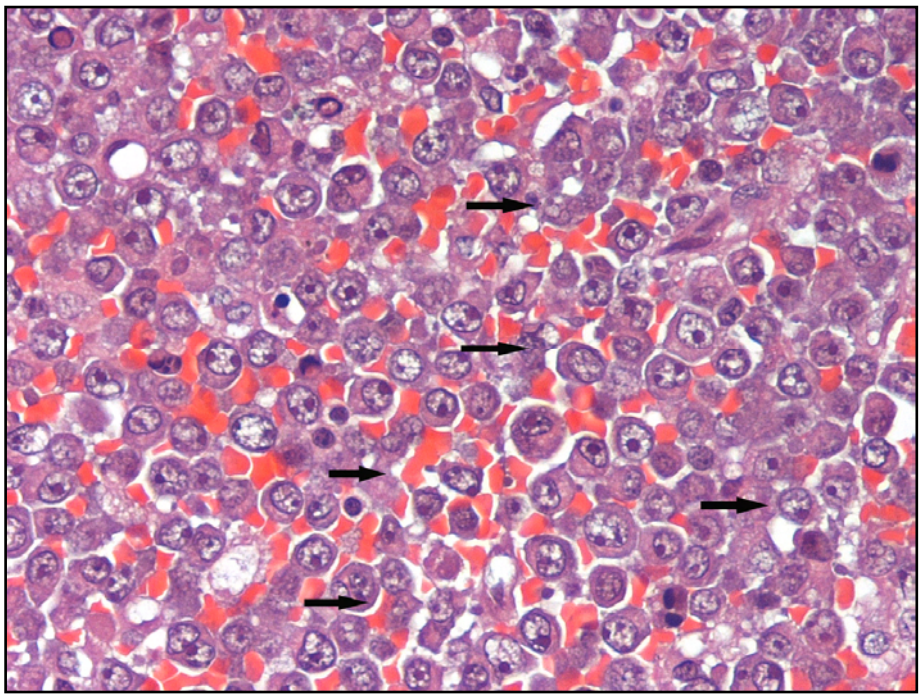

Figure 5: *The micrograph shows a case of PBL with prominent pleomorphism demonstrated by binucleate (thin arrow) and multinucleated (thick arrow) lymphoma cells (H&E 2µm section; Original magnification: 400X).*

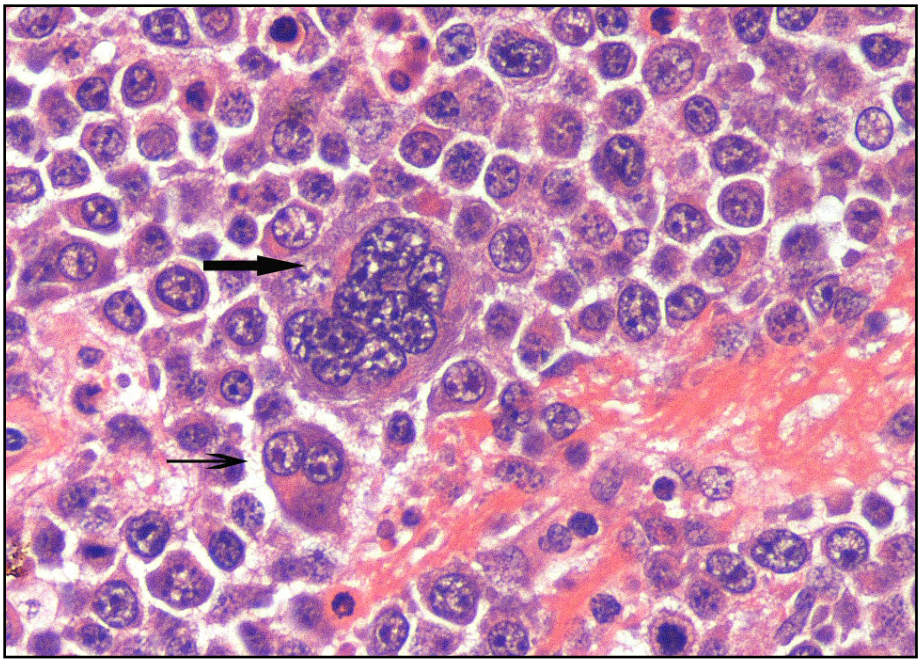

Figure 6: *The micrograph demonstrates the typical 'starry sky' appearance in a case of PBL caused by the presence of numerous tingible body macrophages (arrows) between the tumour cells (H&E 2µm section; Original magnification: 100X).*

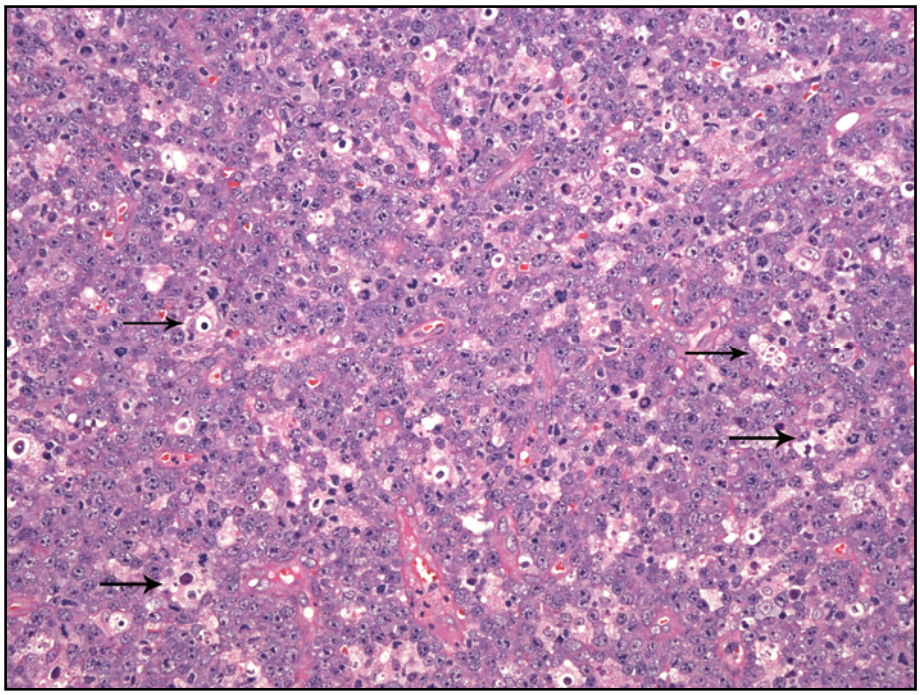

Figure 7: *The micrograph demonstrates a case of PBL with plasmacytic differentiation defined by the presence of more mature plasmacytic cells (arrows) intermingled with the blasts in the background (H&E 2µm section; Original magnification: 400X).*

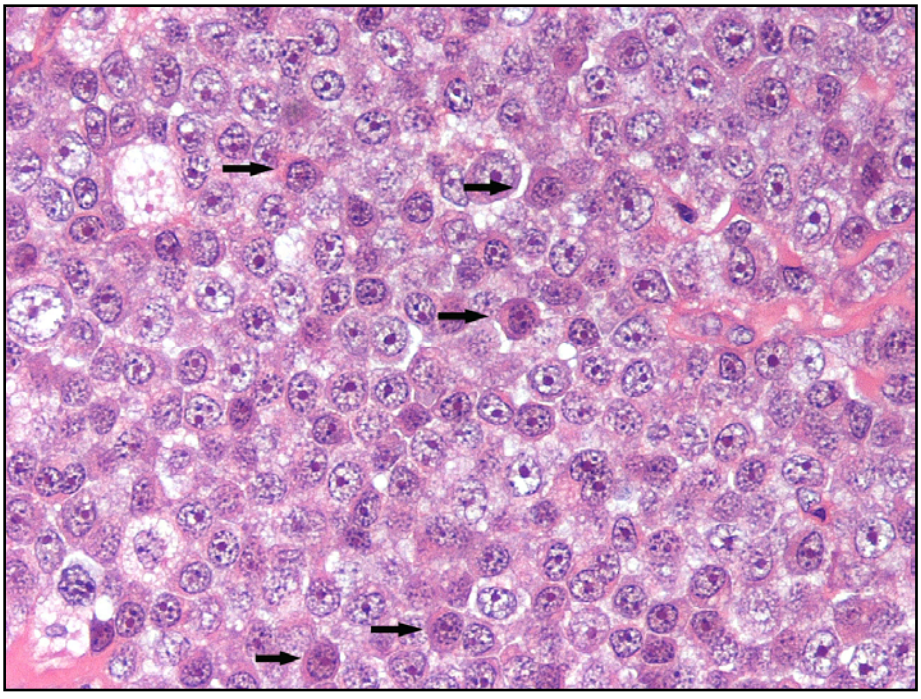

3.3 Immunohistochemistry

3.3.1 CD20 and CD3

All cases of PBL included in this study were uniformly negative for CD20 although some reactive B-cells were always present to serve as a positive internal control (Fig.8). No tumour cells stained with CD3. All CD3-positive cells were interpreted as reactive T-cells. Some cases showed only a few CD3 positive T-cells (Fig.9) whilst others showed many more (Fig.10).

Figure 8: *The micrograph taken from a case of PBL confirms all tumour cells to be CD20 negative although reactive B-cells served as positive internal control (arrow) (CD20 stain; 3µm; Original magnification: 400X).*

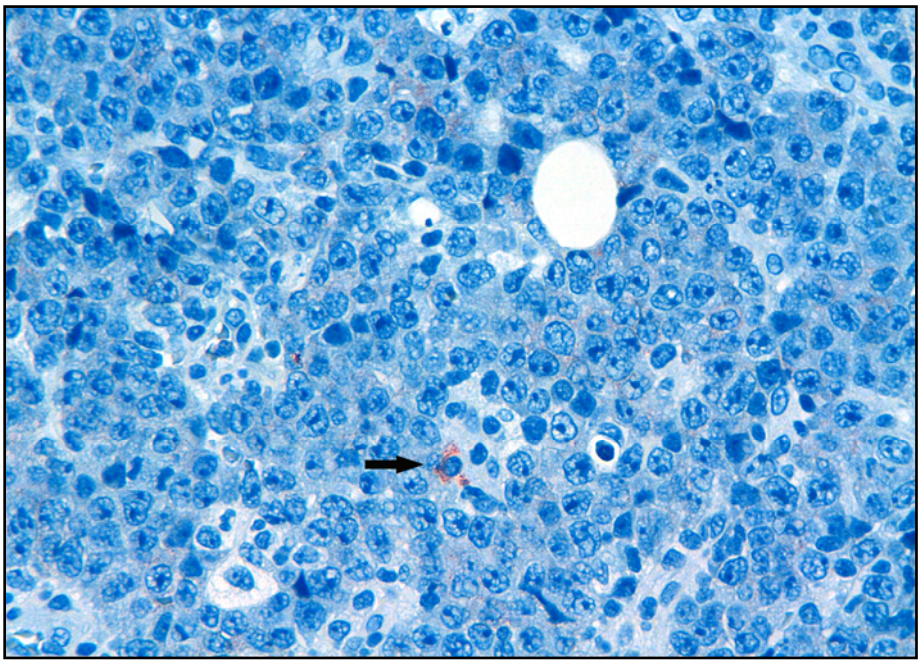

Figure 9: *The micrograph was taken from a case of PBL and confirms all the tumour cells to be CD3 negative. Reactive T-cells (arrows) served as a positive internal control for the CD3 stain (CD3 stain; 3µm; Original magnification: 400X).*

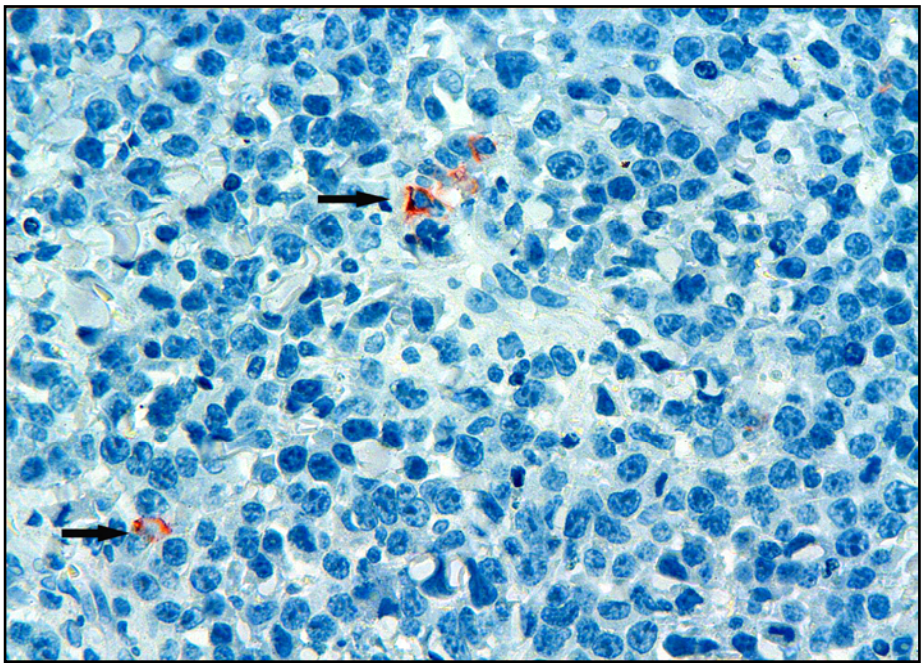

Figure 10: *The micrograph was taken from a case of PBL again confirming the tumour cells to be CD3 negative. More abundant reactive T-cells staining positive with CD3 (arrows) is however present (CD3 stain; 3µm; Original magnification: 400X).*

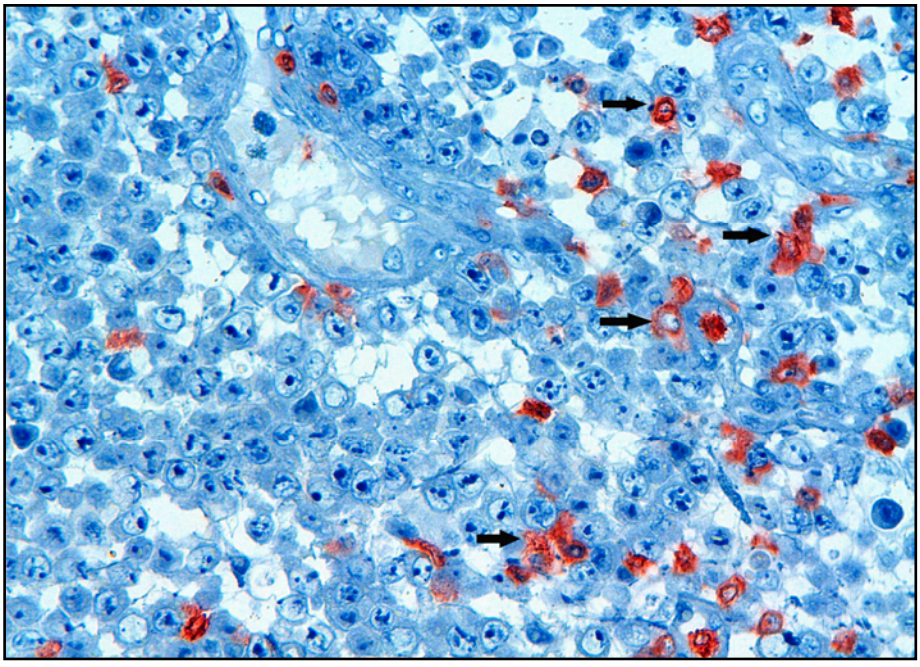

3.3.2 Ki-67

Diffuse and strong positive staining was found with Ki-67 in 34/45 (76%) of cases (Fig.11), intermediary positivity was found in the tumour cells of 9/45 (20%) and in 2 cases (4%) (Cases 17 and 24) positive staining was only focally present in some of the tumour cells (Fig.12).

Figure 11: *The micrograph represents a PBL case with typical diffuse and strong, red-brown positive nuclear staining for the proliferation marker, Ki-67 (Ki-67 stain; 3µm; Original magnification: 100X).*

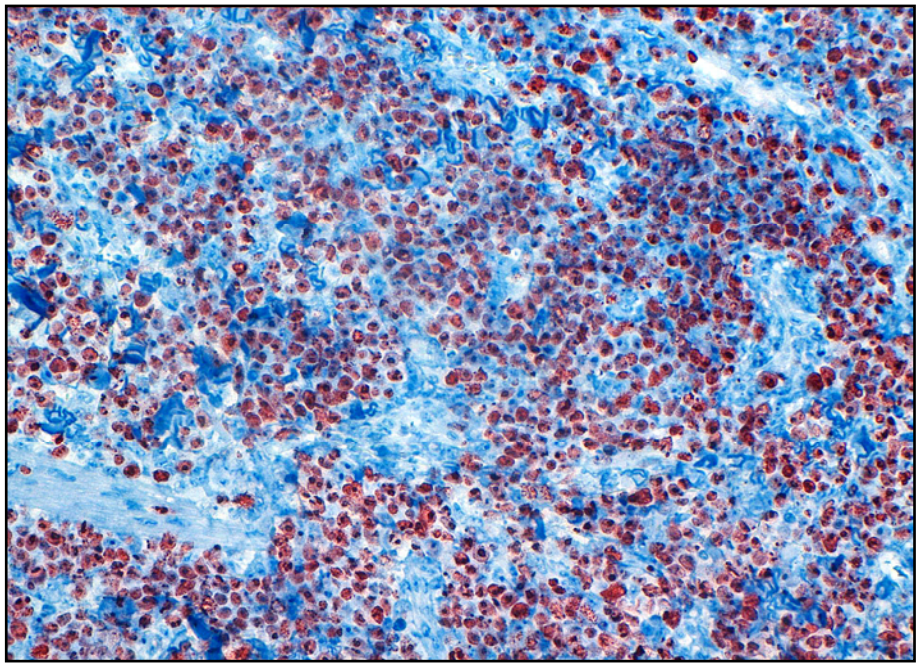

Figure 12: *A micrograph of case 17 showing only focal positivity for Ki-67. (Ki-67 stain; 3µm; Original magnification: 200X).*

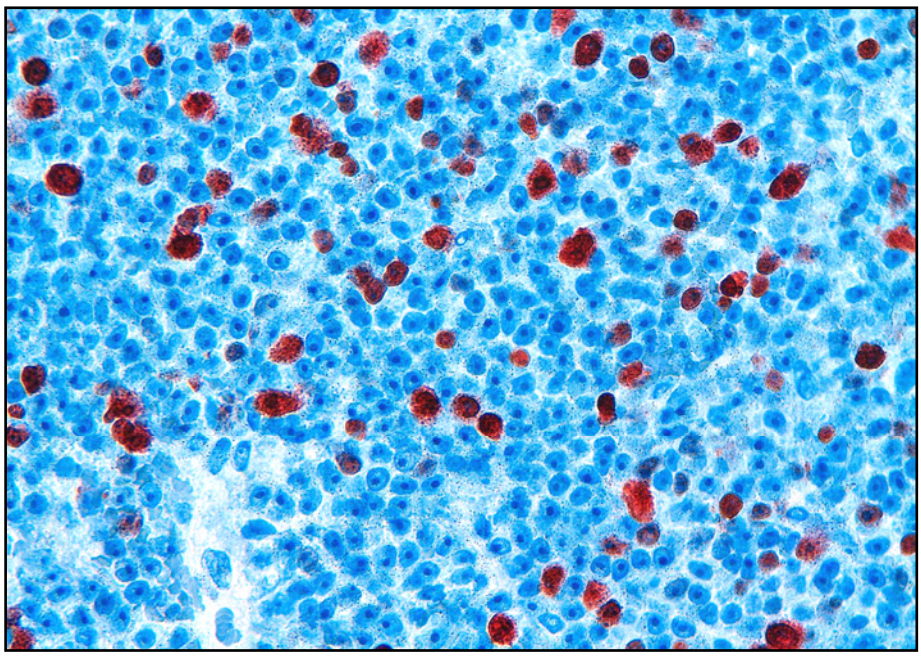

3.3.3 Multiple Myeloma oncogene-1 (MUM1)

In the case of MUM1, 39/45 (87%) of cases showed strong and diffuse staining of the tumour cells (Fig.13), 5/45 (11%) showed positivity in only an intermediary number of the cells whilst one case (2%) (Case 43) showed only focal staining with the antibody (Fig.14).

Figure 13: *Strong and diffuse positive cytoplasmic staining with MUM in the tumour cells of a case of PBL (MUM stain; 3µm; Original magnification: 200X).*

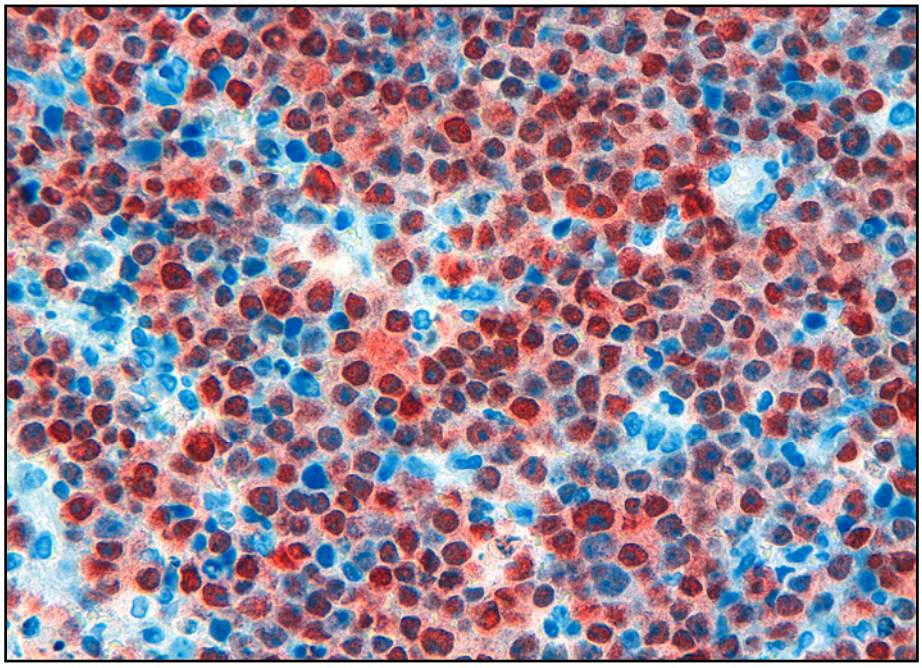

Figure 14: *The micrograph was taken of the MUM stain of case 43. Only focal positivity was present (MUM stain; 3µm; Original magnification: 200X).*

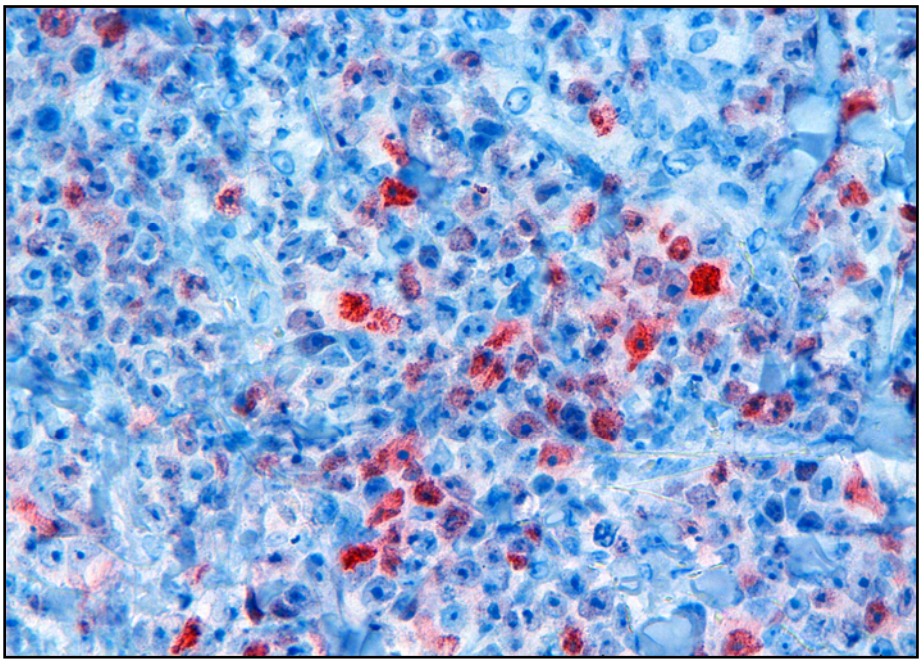

Variable immunoreactivity was found with CD45, CD79a, CD38 and CD138.

3.3.4 CD45

Apart from one case which stained negative for CD45 (Case 42), 44/45 (98%) of cases showed at least some form of positivity with this antibody with 17/45 (38%) showing diffuse and strong positivity (Fig.15).

Figure 15: *Strong positive staining for CD45 is present on the cell membranes of most of the tumour cells in this PBL. Some reactive B- and T-cells are also seen on this micrograph (arrows). (CD45 stain; 3µm; Original magnification: 200X).*

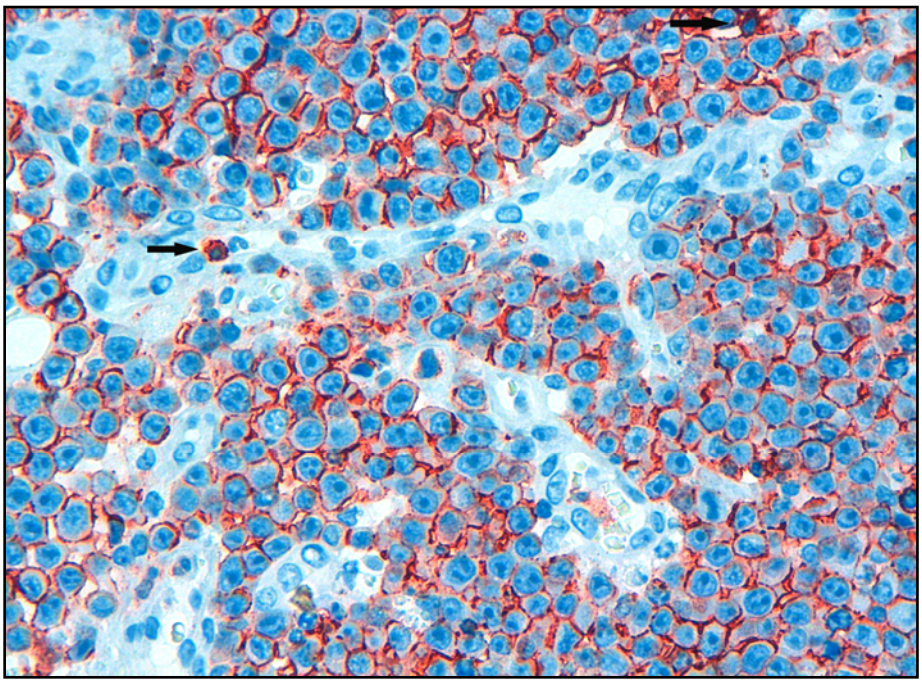

3.3.5 CD79alpha

Not a single case stained diffusely positive for CD79a. Intermediary positivity was seen in only one case (2%) (Case 32) (Fig.16) while 27/45 (60%) of cases showed focal staining only. No staining could be detected in 17/45 (38%) of cases, although strong positivity were present in reactive B-cells on the section (Fig.17) which served as internal control for this immunohistochemical stain. Overall, only 62% of cases showed some positive staining for this B-cell marker.

Figure 16: *Red-brown granular staining for CD79a is seen in the cytoplasm of the tumour cells (arrows) in this case of PBL (CD79a stain; 3µm; Original magnification: 200X).*

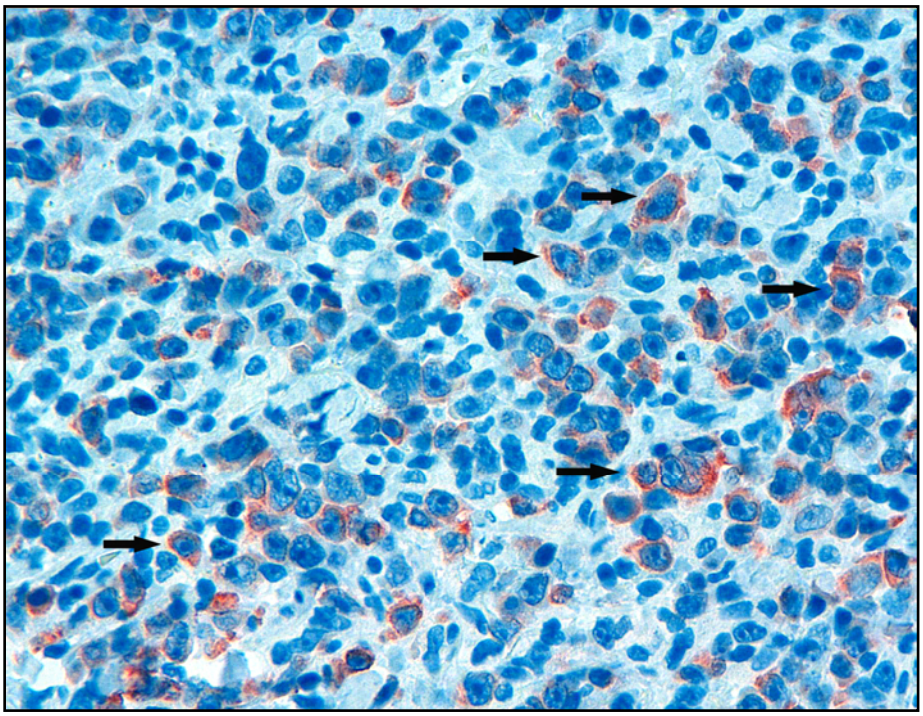

Figure 17: *The micrograph represents a case of PBL where positive staining for CD79a is seen in only the reactive B-cells (arrows) but not in the tumour cells (CD79a stain; 3µm; Original magnification: 200X).*

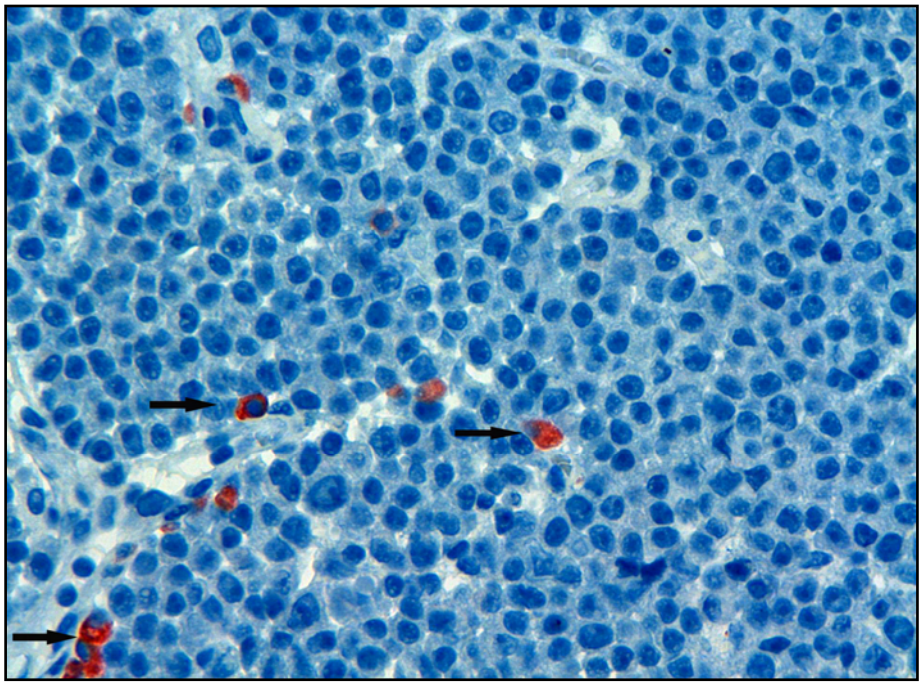

3.3.6 CD38

The plasma cell marker CD38 showed no staining in 16/45 (36%) of cases while 15/45 (33%) showed focal staining in the tumour cells, 7/45 (16%) showed positive staining in an intermediary number of cells and 7/45 (16%) cases showed diffuse positivity for this marker (Fig.18). Strong positivity was always present in reactive plasma cells which served as positive internal control for CD38 negative cases (Fig.19).

Figure 18: *The micrograph shows diffuse positive CD38 staining on the cell membranes of the tumour cells of this case of PBL. Membranous staining clearly delineates the cell membranes of some of the tumour cells (arrows) (CD38 stain; 3µm; Original magnification: 200X).*

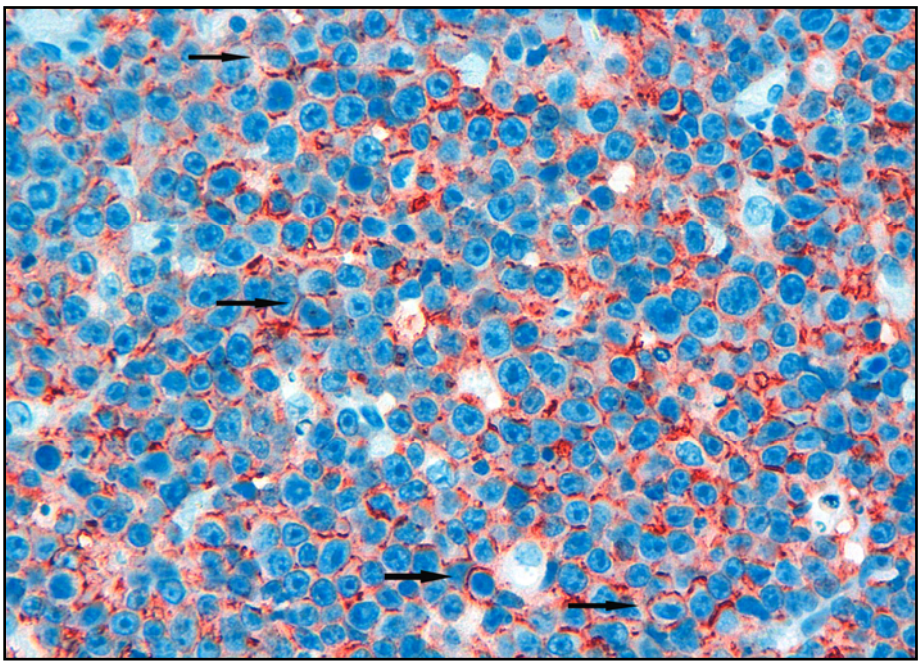

Figure 19: *Positive staining for CD38 is seen as red-brown granular staining in the reactive plasma cells (arrows). None of the larger tumour cells stained positive for CD38 in this case of PBL (CD38 stain; 3µm; Original magnification: 200X).*

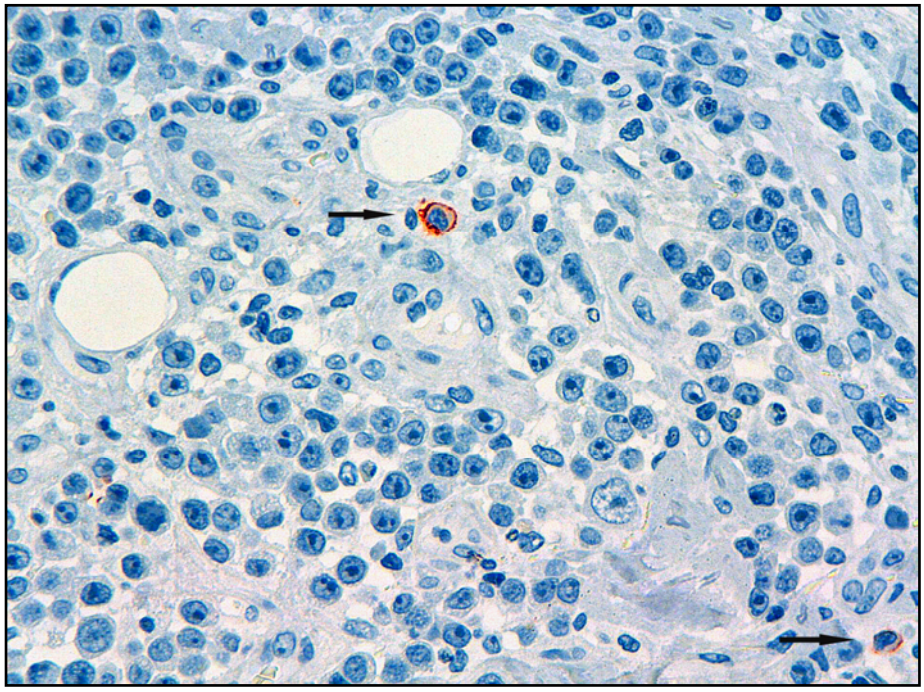

3.3.7 CD138

CD138, another plasma cell marker, showed no staining in 7/45 (16%) of cases, focal staining in 22/45 (49%), intermediary number of cells in 7/45 (16%) and diffuse staining in 9/45 (20%) of cases (Fig.20). All cases negative for CD138 always showed strong positivity in reactive plasma cells (Fig.21) as well as overlying squamous epithelial cells which served as positive internal control for all cases (Fig.22).

Figure 20: *Diffuse positive staining for CD138 is present on the cell membranes of most of the tumour cells in this case of PBL. The membranous stain delineates the cytoplasmic rim of the tumour cells (arrows) (CD138 stain; 3µm; Original magnification: 200X).*

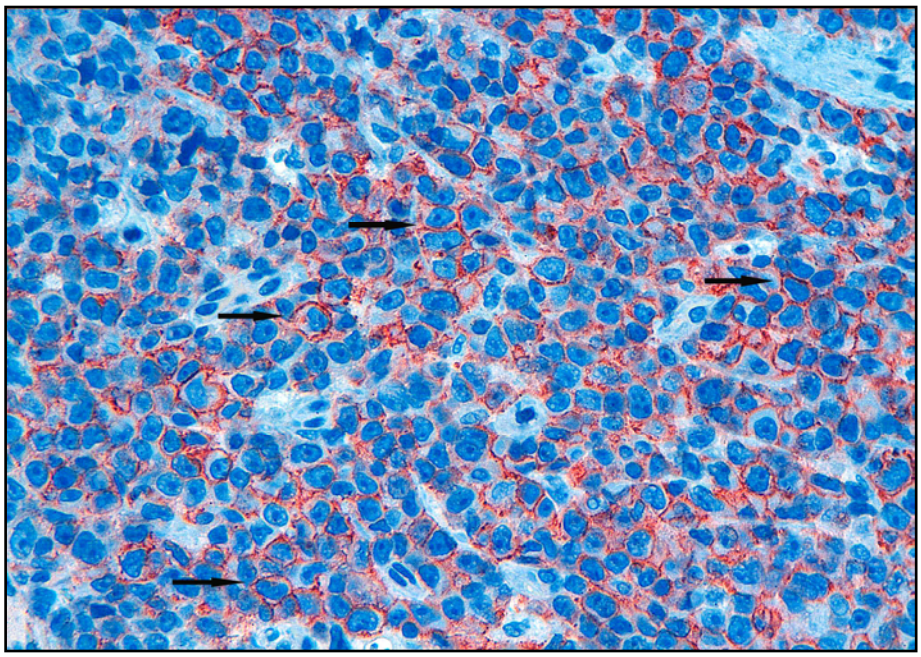

Figure 21: *Positive staining for CD138 is seen only in reactive plasma cells (arrows) of this PBL case. None of the tumour cells stained with this marker (CD138 stain; 3µm; Original magnification: 200X).*

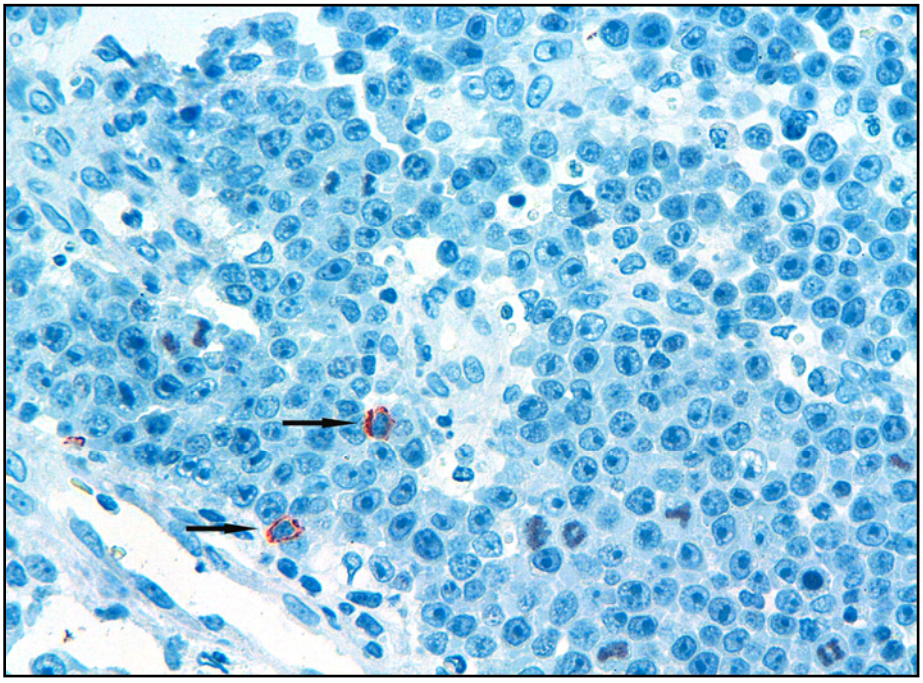

Figure 22: *The micrograph shows a case of PBL that was negative for CD138. Strong positive staining for CD138 is however visible in the basal epithelial cells of the overlying covering epithelium of the oral mucosa (left) (CD138 stain; 3µm; Original magnification: 100X).*

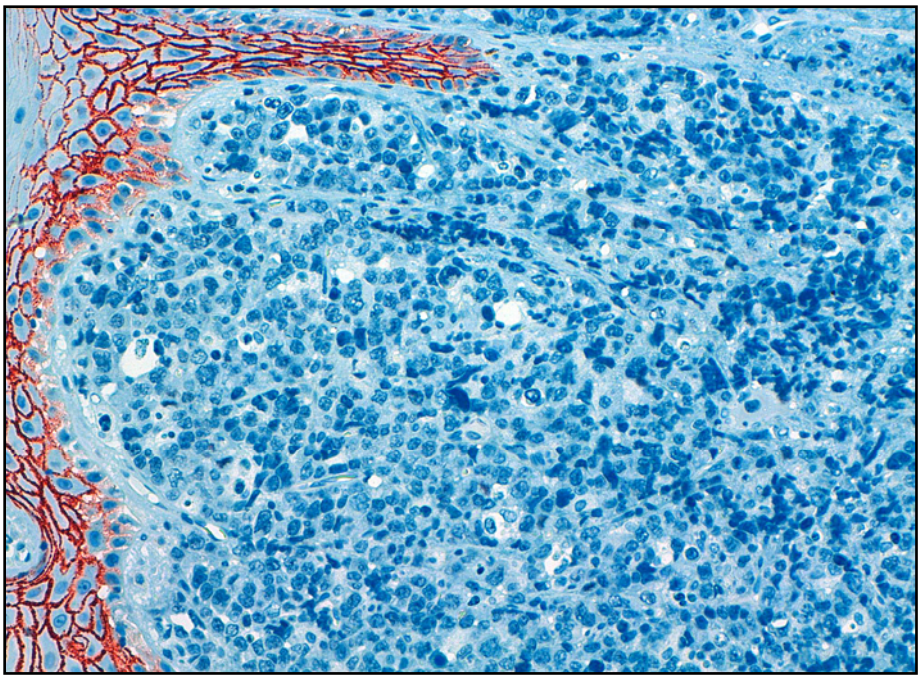

3.3.8 ALK protein

No cytoplasmic ALK protein could be detected in any of the 43 cases of PBL evaluated for the presence of this fusion protein. A case of ALK-positive DLBCL were utilised as positive control and showed strong, red-brown granular staining in the cytoplasm of the tumour cells (Fig.23).

Figure 23: *The micrograph was taken from a case of diffuse large B-cell lymphoma that served as positive control for the ALK protein stain. Red-brown granular staining is seen in the cytoplasm of the tumour cells (ALK stain, 3µm; Original magnification: 200X)*

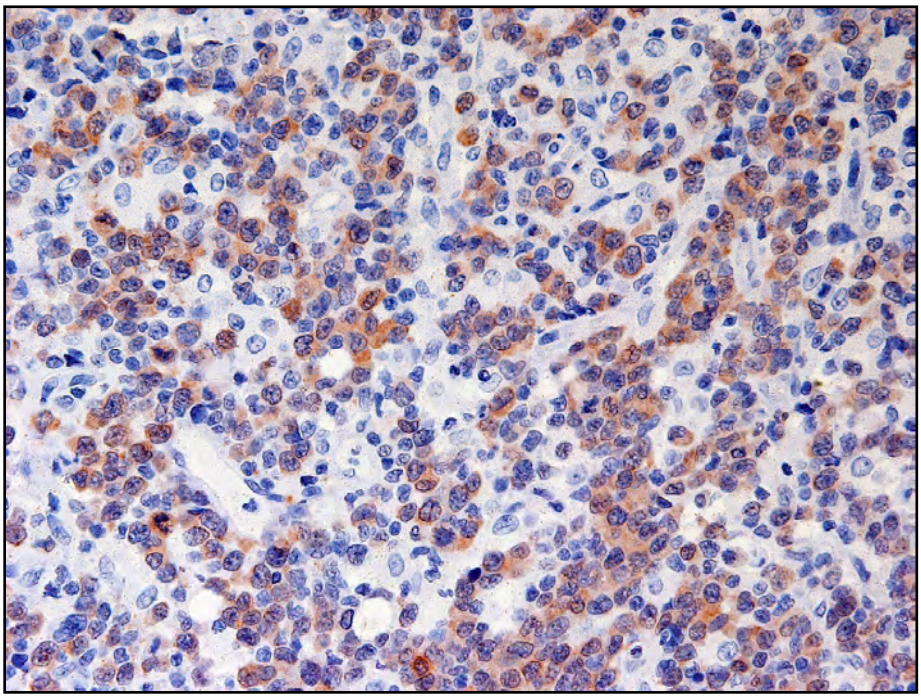

3.3.9 Immunoglobulin light chains

Twenty one of 45 (49%) cases showed light chain restriction with 17/21 (81%) of these cases showing restriction for kappa light chain (Fig.24a) and 4/21 (19%) with lambda light chain restriction. Reactive plasma cells were always present to confirm that negative staining was not aberrantly obtained (Fig.24b).

Figure 24: *This case of PBL shows clear kappa light chain restriction with diffuse red-brown granular cytoplasmic staining for the kappa light chain (a) but with no staining for the lambda light chain (b) in the tumour cells. Reactive plasma cells served at positive internal control in all negative light chain stains (arrow) (kappa (a) and lambda (b) stains; 3µm; Original magnification 200X).*

(a)

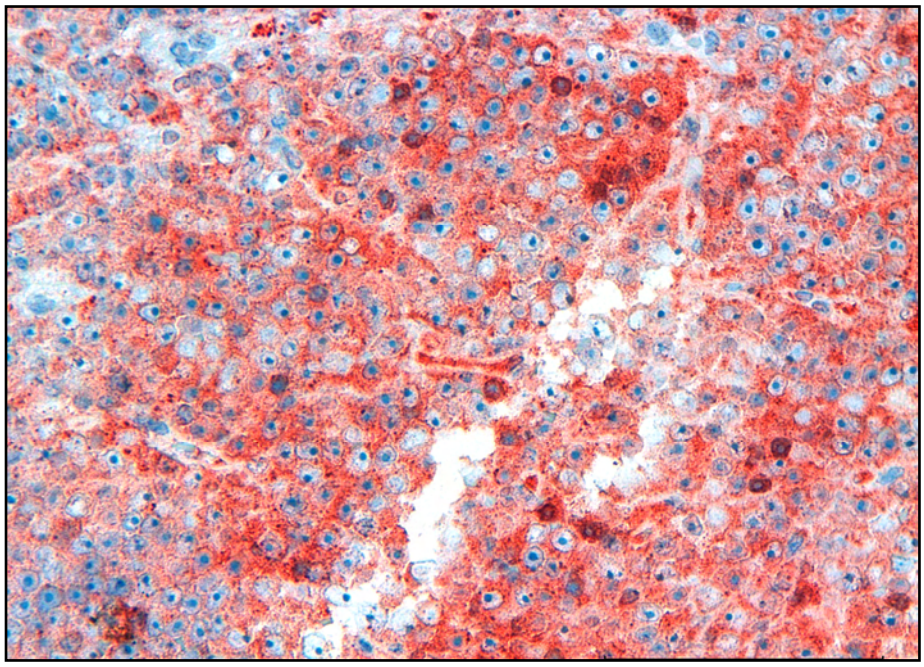

(b)

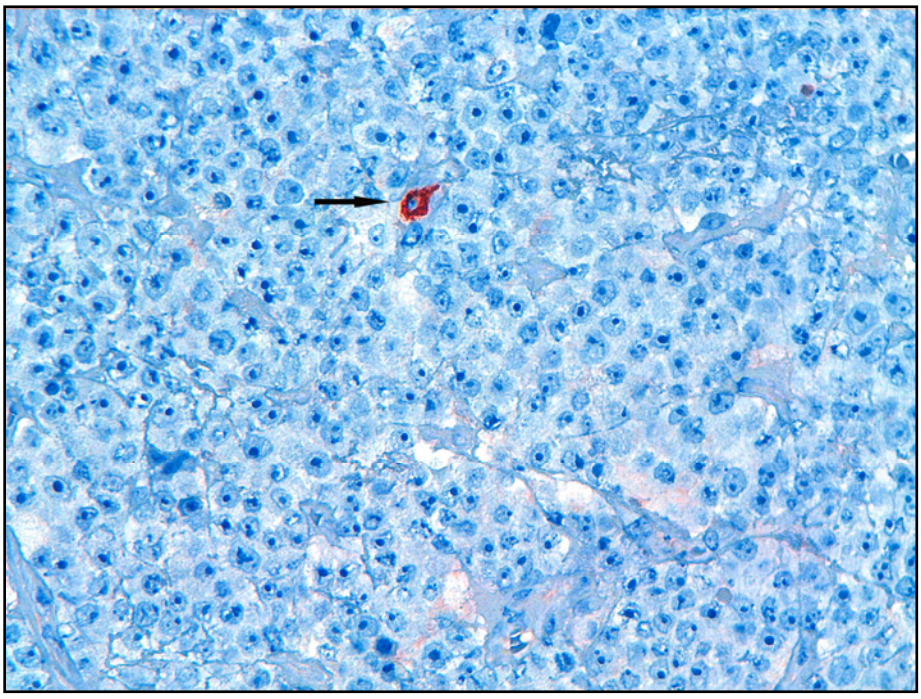

Table 3: *The table represents a summary of the immunophenotypic features of all PBL's included in this study. All cases stained negative for CD3, CD20 and ALK protein (not shown in the table).*

Case	CD45	Ki-67	CD79a	CD38	CD138	MUM-1	K	Λ
1	F	D	F	F	I	D	-	D
2	F	D	F	F	F	I	-	D
3	F	D	F	-	F	D	F	F
4	D	D	-	-	-	D	F	F
5	D	I	-	-	I	D	-	-
6	F	D	-	F	I	I	D	-
7	D	D	-	-	F	D	F	F
8	D	D	F	-	F	D	D	-
9	I	D	F	-	-	D	F	F
10	D	D	F	F	F	I	ND	ND
11	F	D	F	I	F	D	F	F
12	D	D	-	I	D	D	D	F
13	D	I	F	F	I	D	F	F
14	I	D	F	-	-	D	F	-
15	I	D	F	I	F	D	F	F
16	F	D	F	I	D	D	D	F
17	F	F	-	-	D	D	D	-
18	D	D	F	-	F	D	-	F
19	F	D	F	F	-	D	F	F
20	F	I	F	F	D	D	D	F
21	F	I	-	F	I	D	F	F
22	F	I	F	I	F	D	F	-
23	F	I	F	F	D	D	D	-
24	D	F	-	-	F	I	F	D
25	F	D	-	I	F	D	F	-
26	D	D	F	-	F	I	D	F
27	F	D	F	-	F	D	D	-
28	I	D	F	F	I	D	F	-
29	I	D	F	F	-	D	F	F
30	D	D	-	-	-	D	D	-
31	F	D	-	-	F	D	-	F
32	D	I	I	-	F	D	F	-
33	F	D	F	D	I	D	D	F
34	F	D	F	F	F	D	F	D
35	F	D	-	D	D	D	D	-
36	D	D	-	I	-	D	F	-
37	F	I	-	F	F	D	F	-
38	I	D	-	D	F	D	F	-
39	F	D	F	D	D	D	D	F
40	F	I	-	D	D	D	F	F
41	D	D	F	-	F	D	F	F
42	-	D	F	F	F	D	F	-
43	D	D	-	D	F	F	F	-
44	D	D	F	D	D	D	F	F
45	D	D	F	F	F	D	F	F

- = negative; ND = not done; F = focal positive staining (<20% of cells); I = intermediate positive staining (20-70% of cells); D = diffuse positive staining (>70% of cells)

3.4 *In Situ* Hybridisation

3.4.1 Human Herpes Virus-8

Prominent positive staining was evidenced in the Kaposi sarcoma used as positive control for HHV-8 (Fig.25). No positive staining could be found in any of the 45 cases of PBL's evaluated for the presence of this virus.

Figure 25: *The micrograph shows positive, black nuclear staining for HHV-8 (arrows) on the Kaposi sarcoma section hybridised with the HHV-8 probe. This served as positive control for the HHV-8 ISH (ISH for EBV; 3µm; Original magnification: 400X).*

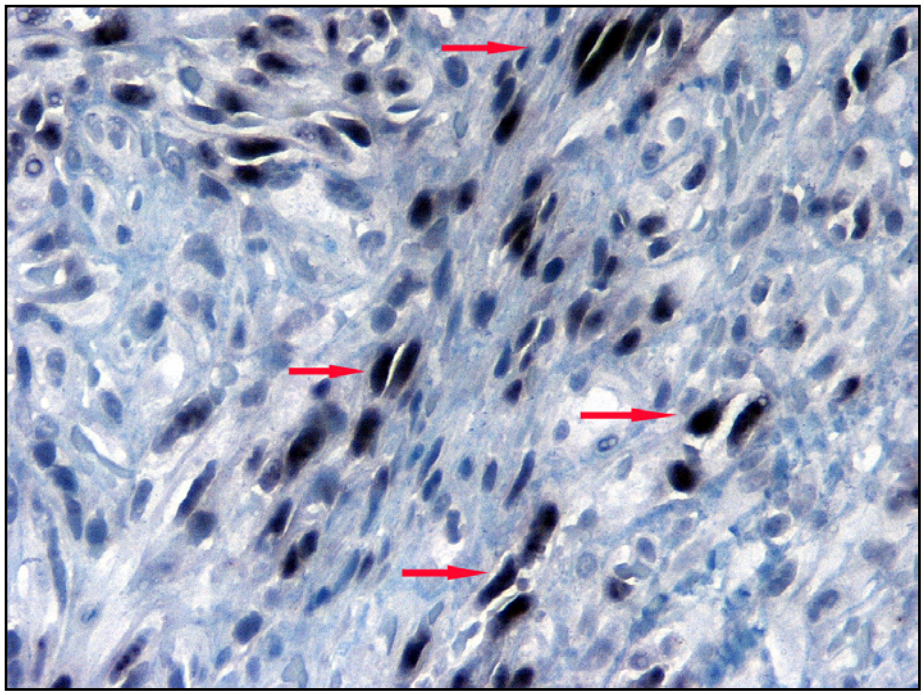

3.4.2 EBV

Forty four (98%) cases showed positive staining for EBV (Fig.26 & 27). The brain sections used as negative controls were always negative for the virus (Fig.28)

Figure 26: *Positive, black nuclear staining for EBV can be seen in many of the tumour cell nuclei on the micrograph of this case of PBL (EBV ISH; 3µm; Original magnification: 200X).*

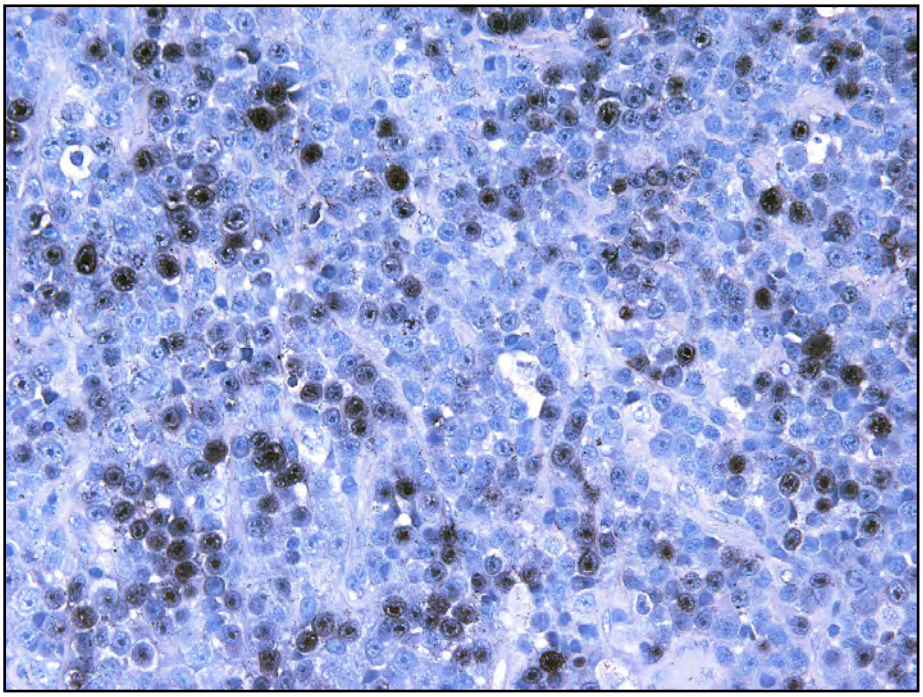

Figure 27: *This is a close-up view to demonstrate the black nuclear staining accepted as positive for EBV ISH (EBV ISH; 3µm; Original magnification: 400X)*

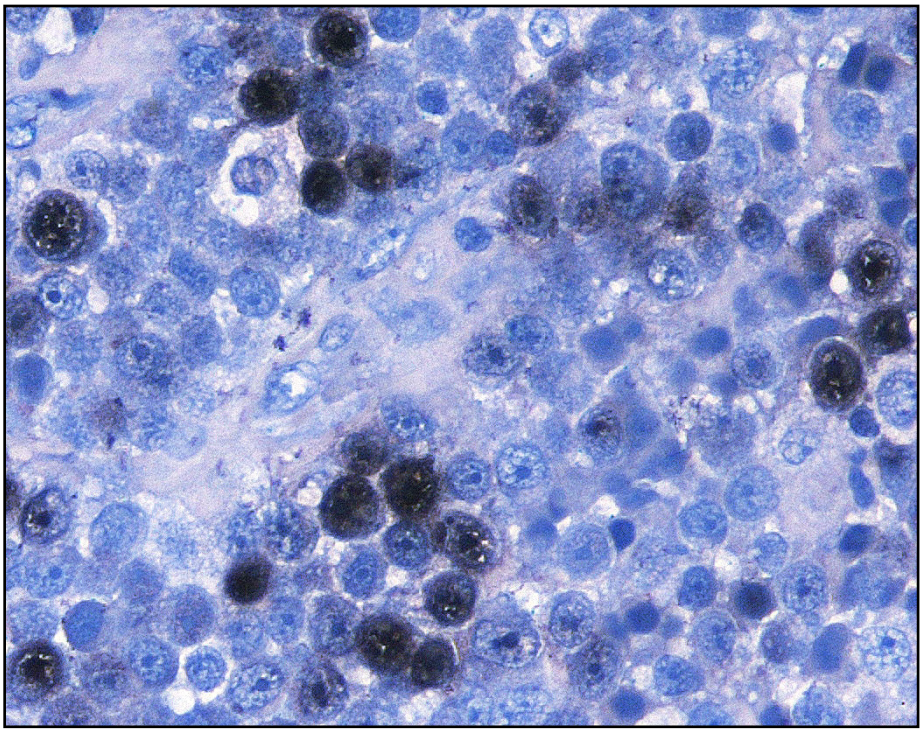

Figure 28: *This micrograph was taken from the brain section that served as negative control for the EBV ISH. No nuclear staining is visible (EBV ISH; 3µm; Original magnification: 400X).*

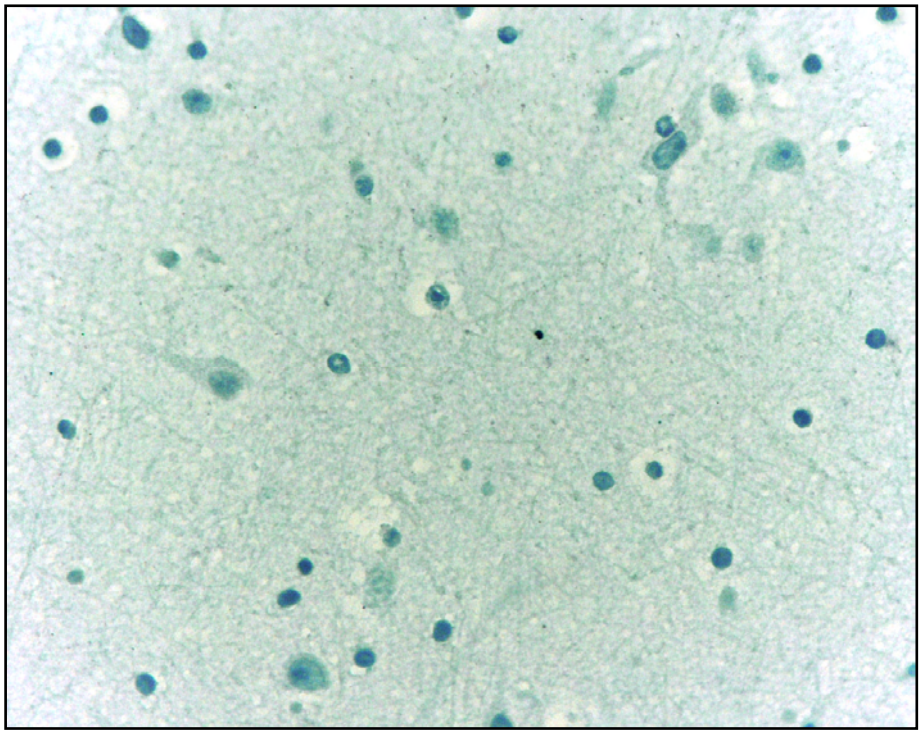

The relationship of EBV and HIV status was analysed (Table 4). The HIV status of only 32/45 (71%) patients were known. Thirty one of these patients with known HIV status were HIV-positive and of these, all were positive for the presence of EBV. Only one patient had a known HIV negative status (Case 17) and in this case no EBV could be demonstrated with ISH.

Table 4: *The table serves as a summary of the HIV, EBV and HHV-8 status of all PBL cases included in this study.*

Case	Age	Sex	HIV	EBV	HHV-8
1	47	M	+	+	-
2	48	M	+	+	-
3	34	F	+	+	-
4	52	F	+	+	-
5	U	M	+	+	-
6	U	U	+	+	-
7	45	F	+	+	-
8	48	M	U	+	-
9	39	F	+	+	-
10	33	F	+	+	-
11	34	M	+	+	-
12	36	F	+	+	-
13	39	M	+	+	-
14	43	M	+	+	-
15	28	F	+	+	-
16	50	M	+	+	-
17	36	F	-	-	-
18	37	M	+	+	-
19	44	M	+	+	-
20	45	M	U	+	-
21	32	F	U	+	-
22	45	M	U	+	-
23	35	M	U	+	-
24	29	M	U	+	-
25	44	M	U	+	-
26	43	M	U	+	-
27	45	M	U	+	-
28	58	F	U	+	-
29	43	M	+	+	-
30	35	M	U	+	-
31	39	M	+	+	-
32	39	M	+	+	-
33	50	M	+	+	-
34	U	U	+	+	-
35	U	M	+	+	-
36	43	M	+	+	-
37	U	M	U	+	-
38	27	M	+	+	-
39	36	M	+	+	-
40	40	M	U	+	-
41	32	M	+	+	-
42	43	M	+	+	-
43	45	F	+	+	-
44	U	F	+	+	-
45	44	M	+	+	-

U = unknown; M = male; F = female; + = positive; - = negative;

3.5 Fluorescence *in situ* hybridisation (FISH)

3.5.1 *IGH* dual colour break apart rearrangement probe (14q32.3 LSI IGH)

FISH analysis with the *IGH* BA probe was performed on the formalin-fixed, paraffin-embedded (FFPE) tissue sections of 43 of the original 45 cases. Cases 1 and 40 did not have adequate tissue to perform FISH analysis and were therefore excluded.

Results for the *IGH*-BA probe are summarised in Table 5. *IGH* gene rearrangements were found in 27/43 (63%) of PBL cases screened with the *IGH*-BA probe (Fig.31). Seven of these cases were also found to have rearrangements affecting both *IGH* alleles, considered as double hit rearrangements on *IGH* BA (Figs.32 and 33). A high degree of intra-tumour heterogeneity and complexity were seen.

Figure 29: *DAPI stained interphase nuclei of a PBL case hybridised with the LSI IgH dual colour BA rearrangement probe (Vysis®, Abbot Laboratories) showing no BA. Two yellow fusion signals are seen per cell nucleus (yellow arrows). Spectrum orange represents the 3' probe and spectrum green represents the 5' probe, which covers almost the entire variable region of the IGH gene.*

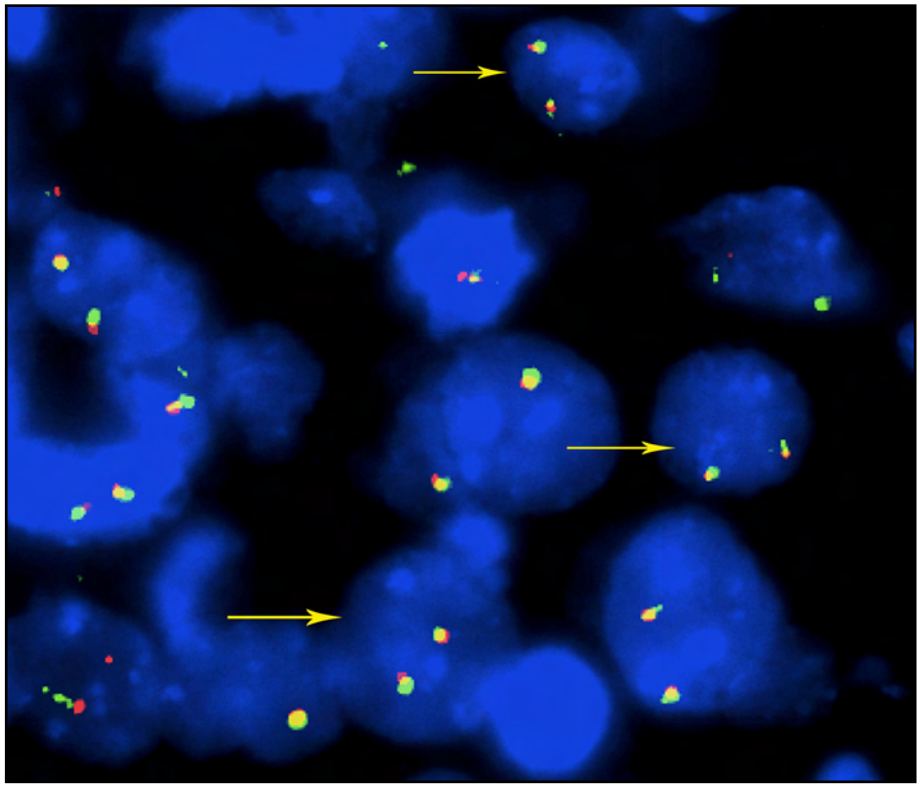

Figure 30: *DAPI stained interphase nuclei of a PBL case hybridised with the LSI IgH dual colour BA rearrangement probe (Vysis®, Abbot Laboratories). Two yellow fusion signals are present in most cell nuclei and no break apart was present in this case. The arrow demonstrates an area of overlapping cell nuclei which created the impression of three fusion signals in one cell. FISH analysis was therefore always performed in single cell nuclei only.*

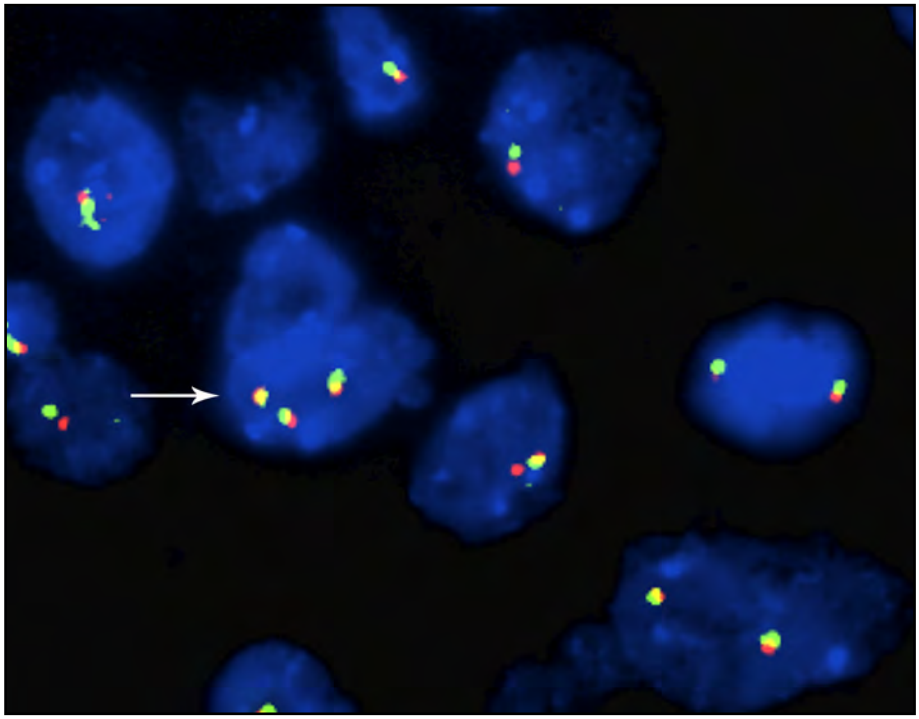

Figure 31: *DAPI stained interphase nuclei of a PBL case hybridised with the LSI IgH dual colour BA rearrangement probe (Vysis®, Abbot Laboratories). IGH rearrangement of one allele is present in some cell nuclei represented as one orange (3') (red arrows) and one green (5') (green arrows) signal apart from each other. The unaffected allele on chromosome 14 is seen as one yellow fusion signal (yellow arrow).*

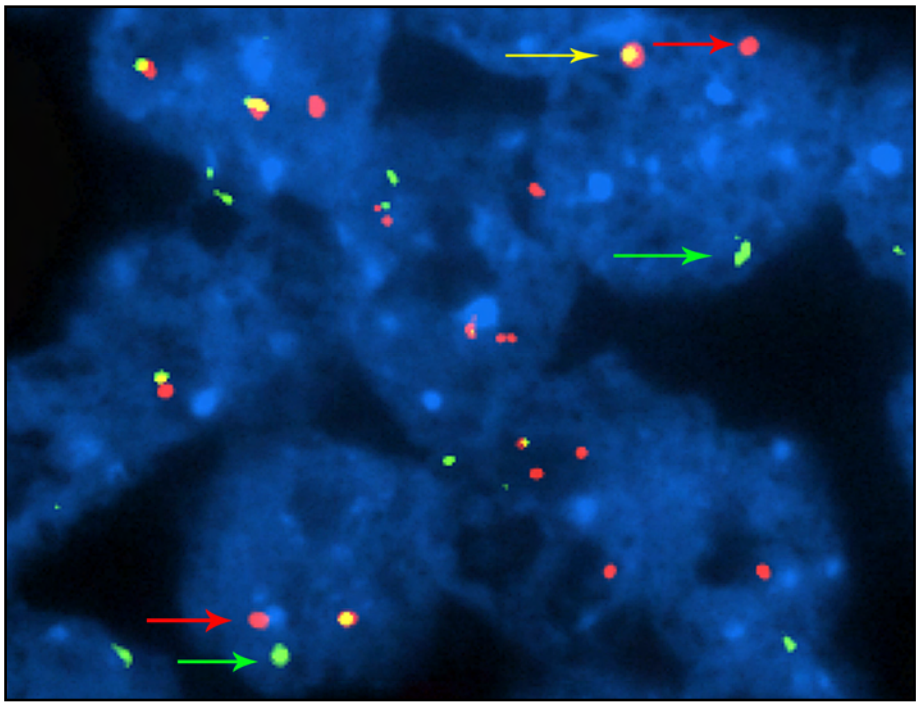

Figure 32: *DAPI stained interphase nuclei of a case of PBL hybridised with the LSI IgH dual colour BA rearrangement probe (Vysis®, Abbot Laboratories) showing IgH rearrangement of chromosomes 14. Two to three copies of orange (3') (red arrow) and one to four copies of green (5') (green arrow) signals are seen in the tumour cell nuclei and there are no normal fusion signals. There are no fusion signals; all IHG copies have a gene rearrangement.*

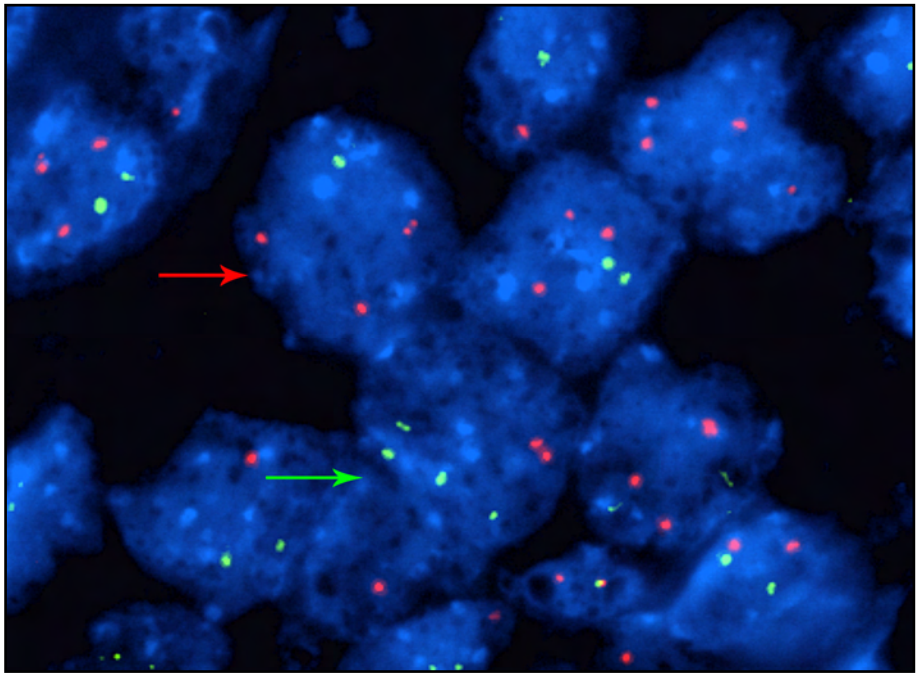

Figure 33: *DAPI stained interphase nuclei of a case of PBL hybridised with the LSI IgH dual colour BA rearrangement probe (Vysis®, Abbot Laboratories) showing IgH rearrangement affecting both alleles on chromosome 14. More than three orange (3') (red arrow) and one to three green (5') (green arrow) signals are seen in the tumour cell nuclei signalling additional copies of IGH. No normal fusion signals are visible in any nucleus.*

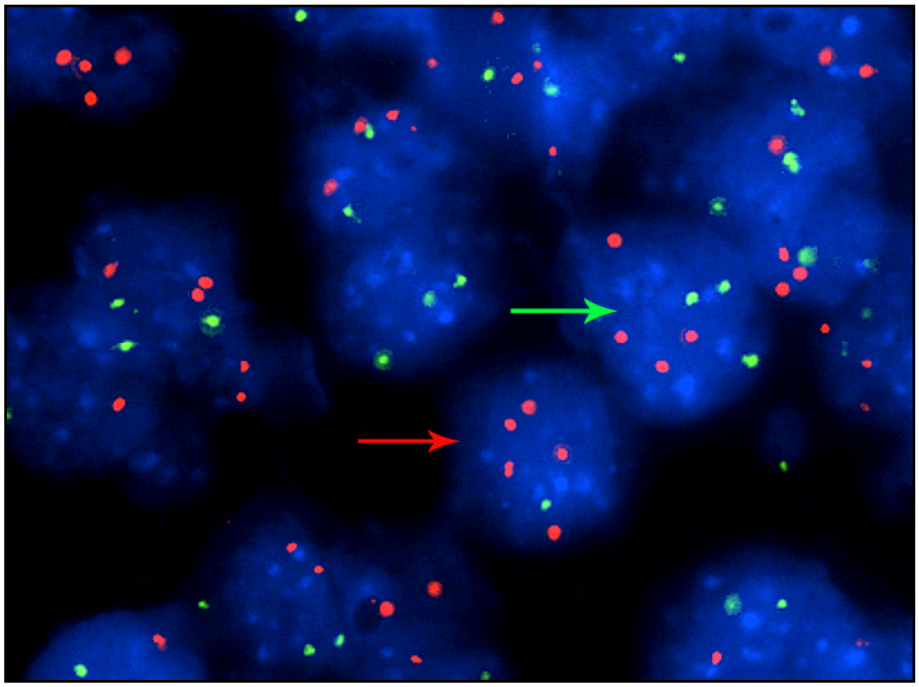

3.5.2 *IGH/MYC*, CEP 8 tri-colour, dual fusion translocation probe [t(8;14)(q24;q32)]

Analysis with the *IGH/MYC* tri-colour, dual fusion translocation probe followed the *IGH*-BA probe in order to see if the *MYC* gene (chromosome 8) was a partner for the *IGH* gene (chromosome 14) in cases positive for *IGH*-BA. The probe could also be used to evaluate chromosome 8 aneuploidy with the centromere 8 enumeration probe. The probe was applied to the FFPE tissue sections of the same cases of PBL analysed with the *IGH*-BA probe. Again cases 1 and 40 were excluded from the analysis. The results for the *IGH/MYC* probe are summarised in Table 5. Twenty-two of 43 PBL cases (51%) were positive for the I*GH/MYC* translocation (Fig.35). A high degree of intra-tumour heterogeneity and complexity were seen.

Figure 34: *DAPI stained interphase nuclei of case 6 hybridised with the MYC/IGH dual colour dual fusion translocation probe (Vysis®, Abbot Laboratories). The nuclear signals represent a normal pattern with two spectrum aqua (chromosome 8 CEP), two spectrum orange (MYC-gene), and two spectrum green (IGH-gene) signals per cell nucleus (arrows). No yellow fusion signals indicative of a t(8;14) are visible here.*

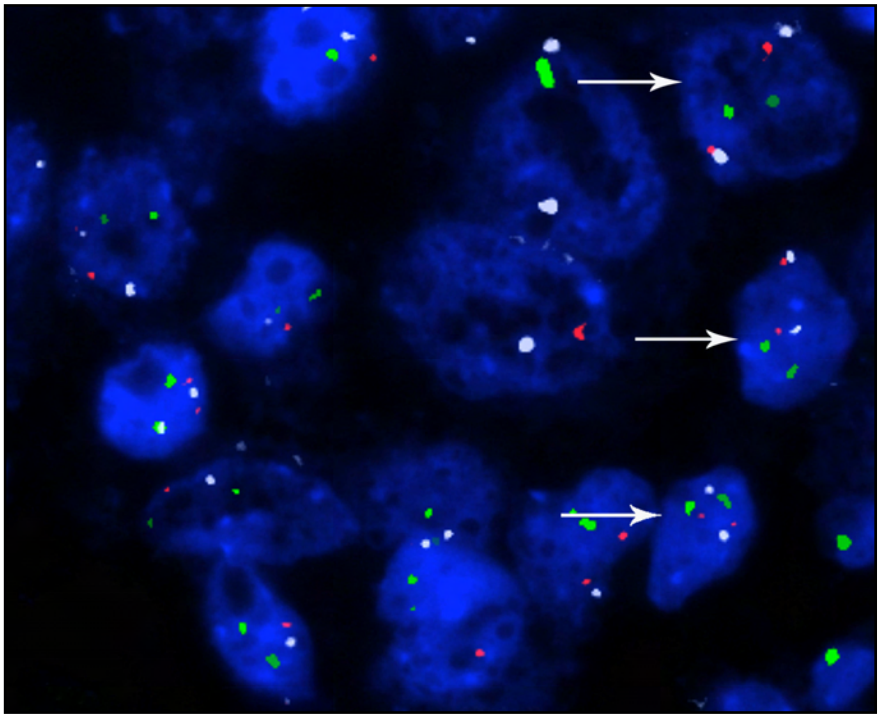

Figure 35: *DAPI stained interphase nuclei of case 2 hybridised with the MYC/IGH dual colour dual fusion translocation probe (Vysis®, Abbot Laboratories). Positive t(8:14) translocation is demonstrated by the positive yellow fusion signals (yellow arrows). The presence of one fusion signal in many cells likely reflects the loss of one translocation derivative (pink arrow). Orange signals represent the MYC gene on chromosome 8 and the green signals represent the IGH gene on chromosome 14.*

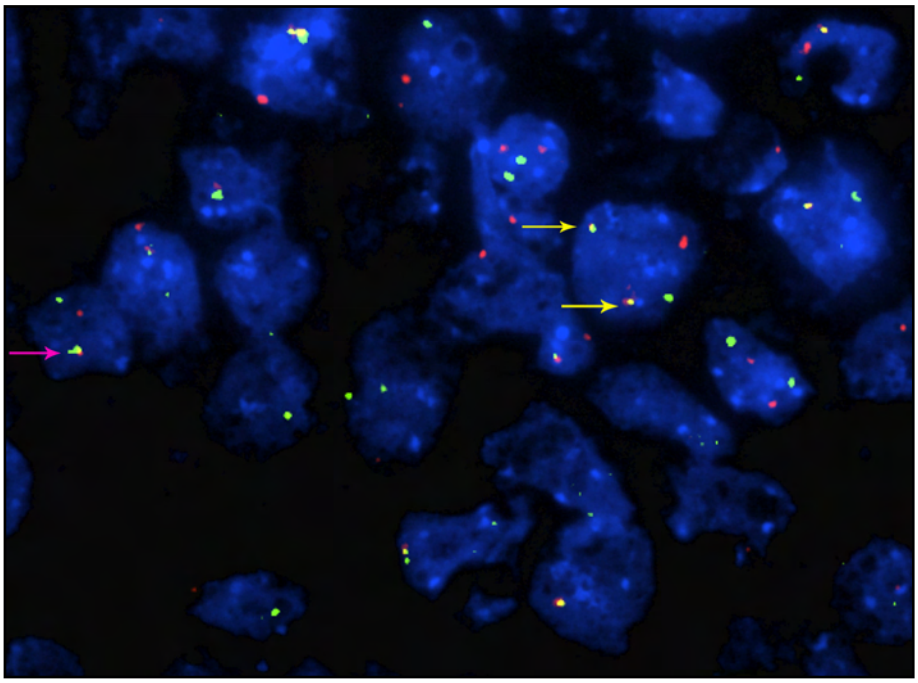

3.5.3 *MYC* dual colour break apart rearrangement probe (8q24 LSI MYC)

The *MYC* dual-colour BA probe was subsequently used to determine if the *MYC* gene was rearranged in cases negative for t(8;14) as the *IgH* BA positive cases would indicate a variant Burkitt translocation. Unfortunately case 13 was negative for *IGH*-BA and t(8;14) but *MYC*-BA was not performed. Twenty cases of PBL were screened with the *MYC*-BA probe. The results for the *MYC* BA probe are summarised in Table 5. Four of 20 (20%) cases (Cases 11, 16, 35 and 37) showed a positive BA signal of the *MYC* probes set (Fig.36). *MYC* was therefore rearranged in 26/42 (62%) of PBL's evaluated in this study (excluding case 13). *IGH* was a partner in 22/42 cases (52%) suggesting that *MYC* was translocated to partners other than *IGH* in four cases.

Interestingly case 16 was positive for both *MYC* and *IGH BA* probes set but were negative for t(8;14).

Figure 36: *DAPI stained interphase nuclei of case 11 hybridised with the LSI MYC dual colour BA rearrangement probe (Vysis®, Abbot Laboratories) showing MYC rearrangement of one allele as one spectrum orange (5') and one spectrum green (3') signal (arrows) apart from each other. The normal yellow fusion signal represents the unaffected allele on chromosome 8.*

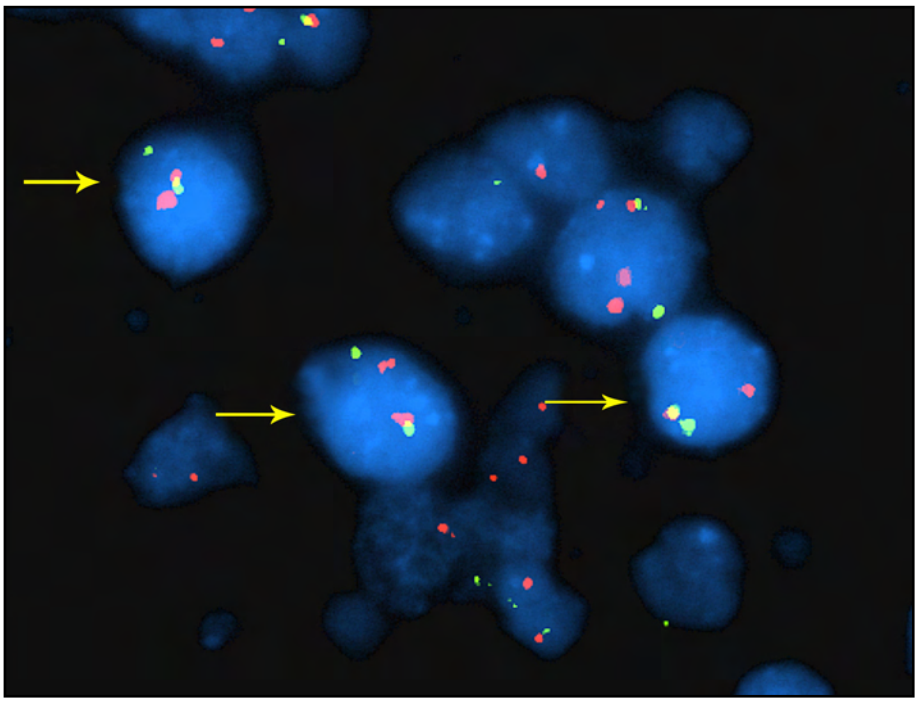

3.5.4 *IGH/CCND1* dual colour, dual fusion translocation probe [t(11;14)(q13;q32)]

Forty one of the PBL cases in this study were screened for t(11;14). Cases 1, 23, 40 and 44 were excluded due to inadequate tissue for analysis.

The results for the *IGH/CCND1* probe are summarised in Table 5. The *CCND1* gene was found to be involved in a translocation with *IGH* in only one of 41cases (case 27) (5%) (Fig.37). Increased *CCND1* copy number (orange signals) was however present in 17/41 (41%) cases screened with the t(11;14) probe. This was defined as three or more orange signals per nucleus. Seven cases had more than six copies (cases 4, 8, 14, 21, 29, 38 & 42) (Fig.39) with some having more than 10 signals, noted as "multiple red". Increased *IGH* copy number (green signals) was present in 6/41 (15%) cases screened with this t(11;14) probe set (cases 4, 16, 27, 29, 33 and 38). The high number of green *IGH* signals seen in those cases with *IGH* BA can partly be explained by the fact that there was a split of the green probe spanning

both the 3' and 5' region of *IGH*. In four cases however (cases 4, 16, 27 and 29), cells with more than six copies of *IGH* could be found (Figs. 38 & 39). Cases with more than four signals are representative of a true increase in the copy number of chromosome 14.

Figure 37: *DAPI stained interphase nuclei of complex case 27 hybridised with the IGH/CCND1 dual colour dual fusion translocation probe (Vysis®, Abbot Laboratories). Positive t(11;14) translocation is demonstrated by the positive yellow fusion signals . Two fusion signals are visible in some cells (yellow arrows). Orange signals represent the CCND1 gene on chromosome 11 and the green signals represent the IGH gene on chromosome 14. The IGH gene was also shown to be rearranged on the IGH BA analysis.*

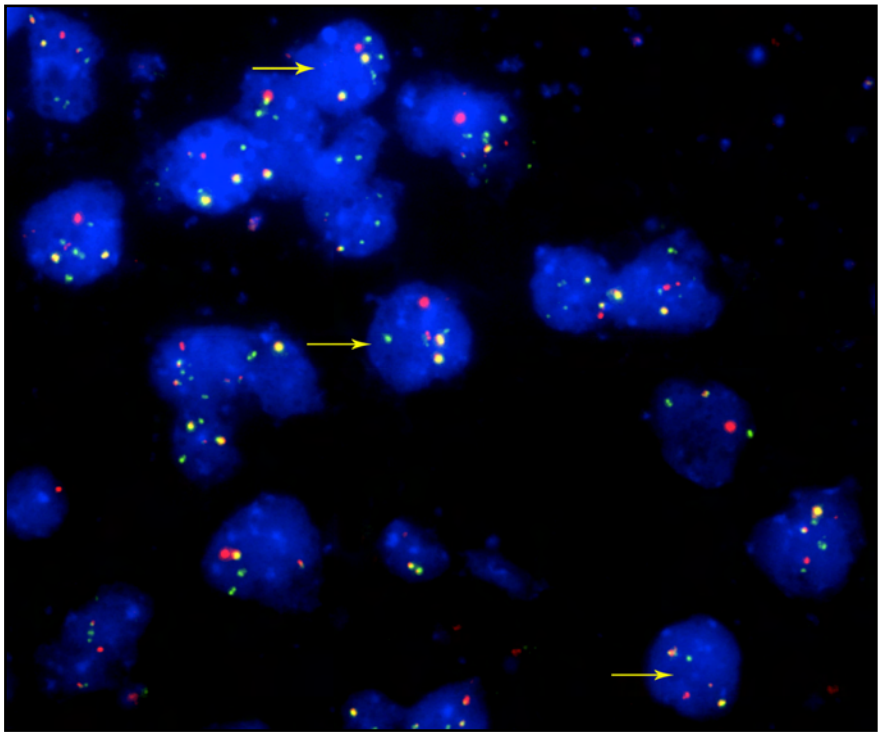

Figure 38: *DAPI stained interphase nuclei of case 7 hybridised with the IGH/CCND1 dual colour dual fusion translocation probe (Vysis®, Abbot Laboratories). Three to six copies of the CCND1 gene on chromosome 11 are represented by the spectrum orange signals (red arrows). A cell with seven green signals, representative of three to four IGH signals on chromosome 14 (green arrow) is also shown here. IGH was also rearranged on the IGH BA probe analysis of this case.*

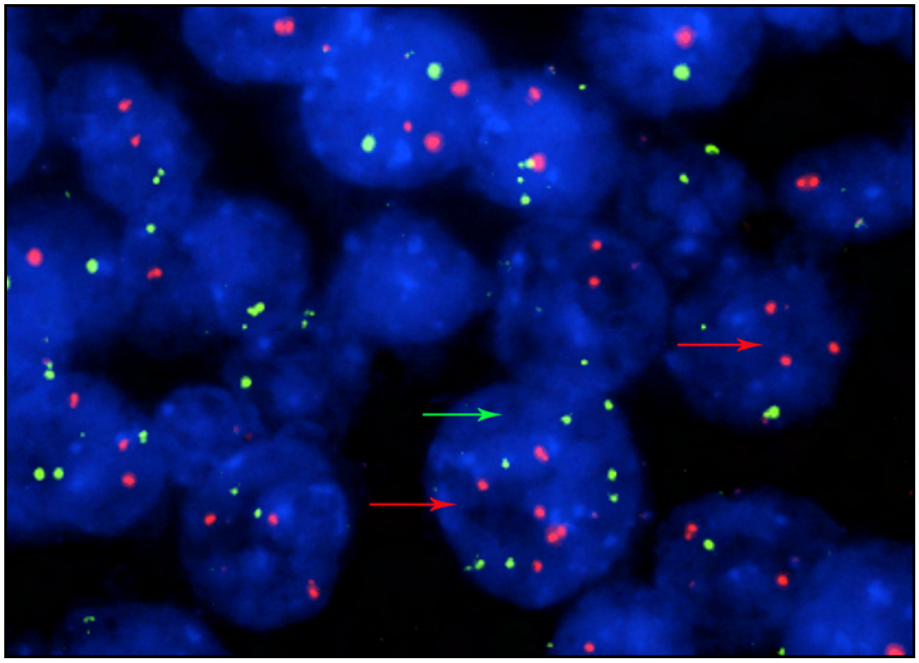

Figure 39: *DAPI stained interphase nuclei of case 38 hybridised with the IGH/CCND1 dual colour dual fusion translocation probe (Vysis®, Abbot Laboratories). Four to ten copies of the CCND1 gene on chromosome 11 are represented by the orange signals (red arrows). Green signals represent the IGH gene on chromosome 14 which also shows an increased copy number with up to 10 copies per nucleus (green arrow). The IGH gene was also rearranged on the IGH BA probe analysis of this case.*

.

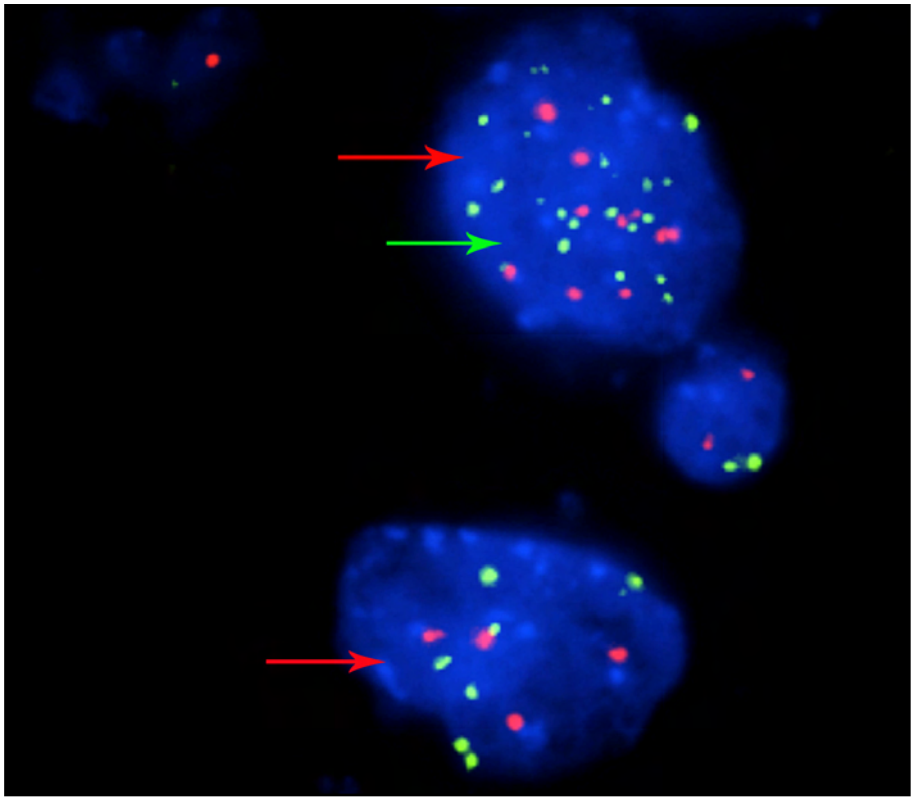

3.5.5 *IGH/BCL2* dual colour, dual fusion translocation probe [t(14;18)(q32;q21)]

The seven PBL with two *IGH* gene alleles rearranged on *IGH* BA probe analysis were screened with the *IGH/BCL2* dual fusion translocation probe in order to evaluate the *BCL2* gene as a possible translocation partner for *IGH*. The results for the *IGH/BCL2* probe are summarised in Table 5. Only case 45 was positive for the t(14;18) translocation.

3.5.6 Double Hit Lymphomas

Seven of the PBL cases included in the study had two *IGH* gene alleles rearranged on *IGH*-BA, and were therefore evaluated as possible double hit lymphomas (Cases 4, 14, 15, 16, 27, 29 and 45) (summarised in Table 5) (Figs. 32 and 33).

In case 27, both the *MYC* and *CCND1* genes were partners of *IGH* genes and positive for t(8;14) and t(11;14) respectively (Fig.37), therefore a true double hit lymphoma case.

In case 45, both *MYC* and *BCL2* genes were discovered to be partners of the *IGH* gene and positive for t(8;14) and t(14:18) respectively, therefore another true double hit lymphoma case

Three cases (4, 15 and 27) were positive for t(8;14) with complex rearrangements of case 4 on t(8;14) (Fig.40). One partner remained unidentified in these three cases;

In cases 14 and 16, both *IGH* chromosome partners remained unknown.

Figure 40: *DAPI stained interphase nuclei of case 4 hybridised with the MYC/IGH dual colour dual fusion translocation probe (Vysis®, Abbot Laboratories). The nuclear signals have a complex pattern with various copy numbers of the the IGH-gene (represented by spectrum green) (green arrows) and two to four yellow fusion signals (yellow arrows) signaling a MYC-IGH translocation. Three CEP 8 signals (represented by spectrum aqua), are seen in some cell nuclei (pink arrows)*

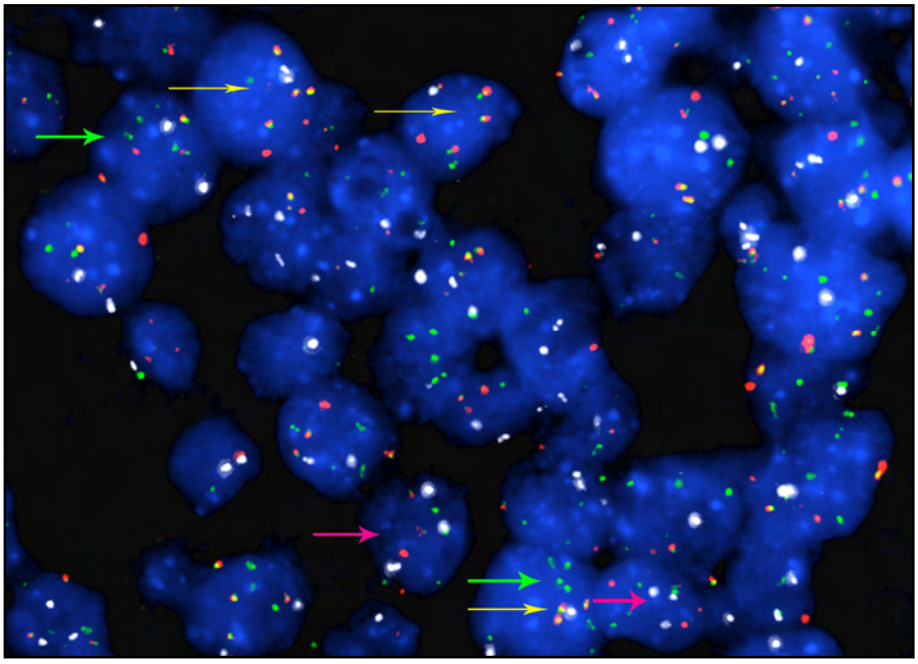

3.5.7 *BCL6* break apart rearrangement probe (3q27)

Forty of the 45 cases were screened for breaks within the *BCL6* gene loci using Vysis LSI dual colour BA rearrangement probes for the *BCL6* locus on chromosome 3 (Abbott Molecular Inc, IL, USA) (cases 1, 4, 6 and 40 were excluded).

The results for the *BCL6* BA probe are summarised in Table 5. No rearrangements of *BCL6* were detected in any of the 40 PBL's screened with the *BCL6* BA probe but gains with three to seven fusion signals per cell were observed in 11 cases (28%) (Fig.41). Loss of fusion signals were seen in three cases (cases 25, 35 and 43) defined as less than two fusion signals per nucleus in more than 15% of cells screened with the *BCL6* BA probe.

Figure 41: *DAPI stained interphase nuclei of case 38 hybridised with the LSI BCL6 dual colour BA rearrangement probe (Vysis®, Abbot Laboratories) showing no rearrangement of the BCL6 gene but with gains of the BCL6 locus represented by three fusion signals in a significant number of the cell nuclei (arrows). Spectrum orange represents the 5' BCL6 probe and spectrum green represent the 3' probe.*

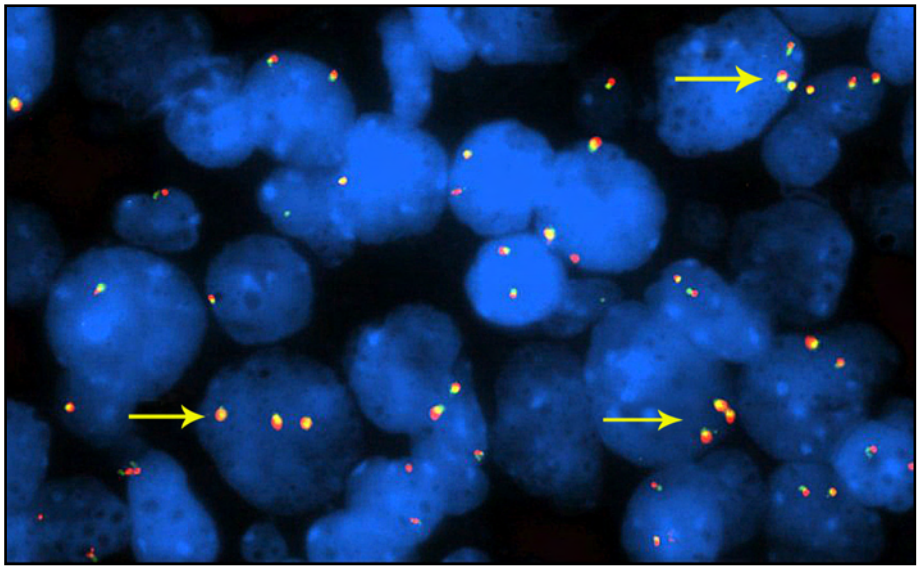

Table 5: *The table provides a summary of the FISH results obtained from this study.*

Case	IGH	MYC/IGH	MYC	t(11;14)	BCL6	t(14;18)
1	ND	ND	ND	ND	ND	ND
2	R	R	ND	-	-	ND
3	R	R	ND	-	-	ND
4	R / DH	R	ND	G (11 & 14)	ND	-
5	R	-	-	-	G	ND
6	-	-	-	-	ND	ND
7	R	R	ND	G (11)	G	ND
8	-	-	-	G (11)	-	ND
9	R	R	ND	G (11)	-	ND
10	R	R	ND	-	-	ND
11	R	-	R	G (11)	-	ND
12	R	R	ND	-	-	ND
13	-	-	ND	-	-	ND
14	R / DH	-	-	G (11)	G	-
15	R / DH	R	ND	-	-	-
16	R / DH	-	R	G (11 & 14)	G	-
17	-	-	-	G (11)	-	ND
18	-	-	-	G (11)	-	ND
19	R	R	ND	-	ND	ND
20	-	-	-	G (11)	-	ND
21	R	R	ND	G (11)	G	ND
22	R	R	ND	-	-	ND
23	-	-	-	ND	-	ND
24	-	-	-	-	-	ND
25	R	R	ND	-	L	ND
26	R	R	ND	-	-	ND
27	R / DH	R	ND	R/G (11 & 14)	-	-
28	R	R	ND	-	-	ND
29	R / DH	R	ND	G (11 & 14)	G	-
30	-	-	-	-	-	ND
31	-	-	-	-	-	ND
32	R	-	-	-	G	ND
33	R	R	ND	G (11 & 14)	-	ND
34	-	-	-	-	-	ND
35	-	-	R	-	L	ND
36	R	R	ND	-	G	ND
37	-	-	R	-	-	ND
38	R	R	ND	G (11 & 14)	G	ND
39	-	-	-	-	G	ND
40	ND	ND	ND	ND	ND	ND
41	-	-	-	G (11)	-	ND
42	-	-	-	G (11)	G	ND
43	R	R	ND	-	L	ND
44	R	R	ND	ND	-	ND
45	R / DH	R	ND	-	-	+

R = positive for rearrangement; - = negative; ND = not done; DH = double hit; G = gain; G (11) = gain of CCND1 on chromosome 11; G (11 & 14) = gain of CCND1 on chromosome 11 and of IGH on chromosome 14; G (14) = gain of IGH on chromosome 14; L = loss

Table 6: *This table provides a summary of the detailed results presented in table 5.*

***IGH*-BA positive**	**Possible double hit on IGH-BA**	**t(8;14) positive**	**t(11;14) positive**	***MYC* BA positive**	**t(14;18) positive**
27/43 screened (63%)	7/43 screened (16%)	22/43 screened (51%)	1/41 screened (2%)	4/20 screened (20%)	1/7 Screened (14%)

Table 7: *The table shows the EBV status of the tumour cells, HIV-status of the patient as well as presence of MYC-rearrangement in every PBL case included in the study.*

Case	HIV	EBV	MYC
1	+	+	ND
2	+	+	R
3	+	+	R
4	+	+	R
5	+	+	-
6	+	+	-
7	+	+	R
8	U	+	-
9	+	+	R
10	+	+	R
11	+	+	R
12	+	+	R
13	+	+	-
14	+	+	-
15	+	+	R
16	+	+	R
17	-	-	-
18	+	+	-
19	+	+	R
20	U	+	-
21	U	+	R
22	U	+	R
23	U	+	-
24	U	+	-
25	U	+	R
26	U	+	R
27	U	+	R
28	U	+	R
29	+	+	R
30	U	+	-
31	+	+	-
32	+	+	-
33	+	+	R
34	+	+	-
35	+	+	R
36	+	+	R
37	U	+	R
38	+	+	R
39	+	+	-
40	U	+	ND
41	+	+	-
42	+	+	-
43	+	+	R
44	+	+	R
45	+	+	-

U = unknown; + = positive; - = negative; ND = not done; R = rearranged

Table 8: *This table represents a summary of the data presented in Table 7 showing the correlation between the EBV statuses and MYC rearrangements in patients with known HIV- status.*

HIV	EBV	*MYC* R	Total patients
+	+	+	18 (58%)
+	+	-	12 (39%)
-	-	-	1 (3%)
			31

+ = positive; - = negative; MYC R = MYC rearranged